AMERICAN SOCIETY FOR MICROBIOLOGY | Journal of Virology®

VACCINES AND ANTIVIRAL AGENTS

Herpes Simplex Virus 1 (HSV-1) 0ΔNLS Live-Attenuated Vaccine Protects against Ocular HSV-1 Infection in the Absence of Neutralizing Antibody in HSV-1 gB T Cell Receptor-Specific Transgenic Mice

Grzegorz B. Gmyrek,[a] Adrian Filiberti,[a] Micaela Montgomery,[b] Alisha Chitrakar,[b] Derek J. Royer,[a] Daniel J. J. Carr[a,b]

[a]Department of Ophthalmology, University of Oklahoma Health Sciences Center, Oklahoma City, Oklahoma, USA
[b]Department of Microbiology and Immunology, University of Oklahoma Health Sciences Center, Oklahoma City, Oklahoma, USA

ABSTRACT The contribution of T cell and antibody responses following vaccination in resistance to herpes simplex virus 1 (HSV-1) infection continues to be rigorously investigated. In the present article, we explore the contribution of $CD8^+$ T cells specific for the major antigenic epitope for HSV-1 glycoprotein B ($gB_{498-505}$, gB) in C57BL/6 mice using a transgenic mouse (gBT-I.1) model vaccinated with HSV-1 0ΔNLS. gBT-I.1-vaccinated mice did not generate a robust neutralization antibody titer in comparison to the HSV-1 0ΔNLS-vaccinated wild-type C57BL/6 counterpart. Nevertheless, the vaccinated gBT-I.1 mice were resistant to ocular challenge with HSV-1 compared to vehicle-vaccinated animals based on survival and reduced corneal neovascularization but displayed similar levels of corneal opacity. Whereas there was no difference in the virus titer recovered from the cornea comparing vaccinated mice, HSV-1 0ΔNLS-vaccinated animals possessed significantly less infectious virus during acute infection in the trigeminal ganglia (TG) and brain stem compared to the control-vaccinated group. These results correlated with a significant increase in gB-elicited interferon-γ (IFN-γ), granzyme B, and CD107a and a reduction in lymphocyte activation gene 3 (LAG-3), programmed cell death 1 (PD-1), and T cell immunoglobulin and mucin domain-containing protein 3 (TIM-3) expressed by TG infiltrating gB-specific $CD8^+$ T cells from the HSV-1 0ΔNLS-vaccinated group. Antibody depletion of $CD8^+$ T cells in HSV-1 0ΔNLS-vaccinated mice rendered animals highly susceptible to virus-mediated mortality similar to control-vaccinated mice. Collectively, the HSV-1 0ΔNLS vaccine is effective against ocular HSV-1 challenge, reducing ocular neovascularization and suppressing peripheral nerve virus replication in the near absence of neutralizing antibody in this unique mouse model.

IMPORTANCE The role of $CD8^+$ T cells in antiviral efficacy using a live-attenuated virus as the vaccine is complicated by the humoral immune response. In the case of the herpes simplex virus 1 (HSV-1) 0ΔNLS vaccine, the correlate of protection has been defined to be primarily antibody driven. The current study shows that in the near absence of anti-HSV-1 antibody, vaccinated mice are protected from subsequent challenge with wild-type HSV-1 as measured by survival. The efficacy is lost following depletion of $CD8^+$ T cells. Whereas increased survival and reduction in virus replication were observed in vaccinated mice challenged with HSV-1, cornea pathology was mixed with a reduction in neovascularization but no change in opacity. Collectively, the study suggests $CD8^+$ T cells significantly contribute to the host adaptive immune response to HSV-1 challenge following vaccination with an attenuated virus, but multiple factors are involved in cornea pathology in response to ocular virus challenge.

KEYWORDS CD8 T cell, HSV-1, eye, interferon, metabolism, transgenic mice, vaccines

Citation Gmyrek GB, Filiberti A, Montgomery M, Chitrakar A, Royer DJ, Carr DJJ. 2020. Herpes simplex virus 1 (HSV-1) 0ΔNLS live-attenuated vaccine protects against ocular HSV-1 infection in the absence of neutralizing antibody in HSV-1 gB T cell receptor-specific transgenic mice. J Virol 94:e01000-20. https://doi.org/10.1128/JVI.01000-20.

Editor Richard M. Longnecker, Northwestern University

Address correspondence to Daniel J. J. Carr, Dan-Carr@ouhsc.edu.

Received 20 May 2020
Accepted 21 September 2020
Accepted manuscript posted online 30 September 2020
Published 23 November 2020

Herpes simplex virus 1 (HSV-1) is a highly successful human pathogen for which well over two billion individuals are seropositive (1–6). While the majority of individuals remain asymptomatic, diseases associated with acute or reactivated virus infection include orolabial lesions, neonatal herpes, herpetic whitlow, encephalitis, and herpetic stromal keratitis (7). More recently, there appears to be a growing body of evidence that in some individuals, HSV-1 may exacerbate or contribute to the development or severity of Alzheimer's disease (AD) (8) or AD-like disease in experimental animal models (9–11). Furthermore, HSV-1 is now recognized as the leading cause of genital HSV infection in western countries (12, 13). Collectively, the spectrum of tissues infected and disease manifestations associated with acute virus infection or reactivation of latent virus that permeates all socioeconomic levels of society demonstrates the need to develop novel treatment modalities to limit the spread of new infections and the incidence of reactivation in those already infected.

Antiviral compounds, including acyclovir and analogues, and additional small molecules that target specific pathways in the replicative cycle of HSV-1 have demonstrated efficacy as potent antiviral molecules but are limited in their application, principally resigned to treat those infected with the virus without changes to the latent virus reservoir (14–18). Another antiviral approach, which involves a novel method that has been found to effectively block viral replication during acute infection or reactivation of latent virus *in vitro*, employs the CRISPR/Cas9 technology (19) to target essential lytic gene expression (20, 21). While this novel technique holds promise and has been used to successfully treat genetic diseases in experimental animal models (22, 23), the successful *in vivo* application of this technology to alter the course of HSV-1 infection has not yet been described.

Clinical vaccine studies have been primarily restricted to genital HSV-2 infection with noted exceptions, all of which have, thus far, failed (24). Previous studies using subunit vaccines against HSV-1 have proven to be effective in experimental mouse models using sterilizing immunity, mortality, and subjective measurements to report tissue pathology as the hallmark of success (25–30). Such subunit vaccinations have yielded neutralizing antibody and the activation of T cells and NK cells associated with the protective effect. Unfortunately, these studies would likely fail similarly to those conducted in HSV-2 clinical trials as a result of targeting primarily glycoproteins of a virus that has developed multiple countermeasures to the host immune system. Other groups have used replication-incompetent virus to demonstrate similar successes with measurable adaptive immune responses in subclinical models as those reported using subunit vaccines (31, 32). Whether such replication-defective virus can induce prolonged antigen expression to elicit a robust immune response with sufficient coverage to multiple antigenic targets has not been adequately evaluated. A final group of viral vaccines that have been reported to show significant efficacy against HSV-1 infection includes those using attenuated viruses constrained by trafficking, cell tropism attenuation, cell fusion, or sensitivity to type I/II interferon (IFN) (33–37). While the immunogenicity of the live-attenuated viruses is evident, the actual antigenic targets that contribute to the success of the vaccine in protecting the host from subsequent infection have not been identified.

We previously reported the use of a live-attenuated virus as a prophylactic vaccine against ocular challenge with the highly neurovirulent strain of HSV-1, McKrae (38). Similar to other studies, we found that the vaccine elicited a robust neutralizing antibody titer but also demonstrated no loss in efficacy in the absence of a functional type I IFN response (39). However, in the absence of T cells, the efficacy of the HSV-1 0ΔNLS vaccine was lost and could only be partially restored with adoptive transfer of $CD4^+$ and $CD8^+$ T cells from HSV-1 0ΔNLS-vaccinated mice (40). As the correlate of protective was found to be antibody-driven, the current study was undertaken to determine if $CD8^+$ T cells are a contributing factor in vaccine efficacy since $CD8^+$ effector T cells have previously been reported to control HSV-1 replication primarily in the trigeminal ganglia (TG) during acute ocular infection and reactivation of latent virus (41–47). The caveat is that the transgenic mice employed in the present study maintain

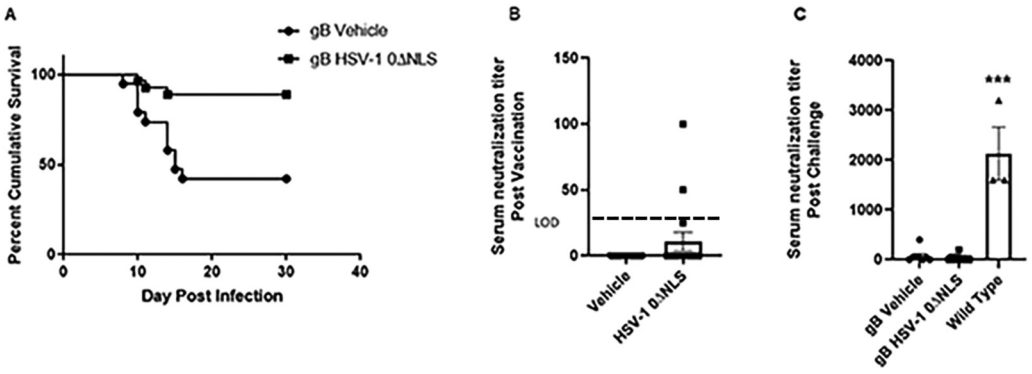

FIG 1 Enhanced survival in the absence of neutralizing antibody in gBT-I.1 transgenic mice vaccinated with HSV-1 0ΔNLS. Male and female gBT-I.1 mice ($n = 19$ to 27/group) were vaccinated and boosted with vehicle or HSV-1 0ΔNLS. Thirty days postboost, serum was collected from anesthetized mice immediately prior to challenge with HSV-1 (10^4 PFU/cornea). (A) Mice were monitored for survival over 30 days postchallenge. **, $P < 0.01$ comparing vehicle- to HSV-1 0ΔNLS-vaccinated mice as determined by Mantel-Cox test. (B and C) Neutralizing antibody titer pre- (B) and post- (C) challenge in vaccinated mice. Data are presented as mean ± SEM taken from three independent experiments. Wild-type is C57BL/6 mice that have survived infection at 1,000 PFU/eye representing vehicle- or HSV-1 0ΔNLS-vaccinated mice. ***, $P < 0.007$ comparing the gBT-I.1 surviving mouse serum neutralization titer compared to wild-type mice as determined by the Kruskal-Wallis nonparametric analysis of variance (ANOVA).

a predetermined population of $CD8^+$ T cells, >85% of which are precommitted to recognition of the HSV-1 peptide, $gB_{495–505}$ (48). By comparison, the frequency of cytotoxic T cells targeting the HSV-1 $gB_{495–505}$ peptide in wild-type C57BL/6 mice is approximately 60 to 75% after HSV-1 exposure (49). In the current study, the generation of neutralizing antibody to HSV-1 following vaccination is found to be nearly absent, but the efficacy of the vaccine in controlling virus replication in the nervous system is not lost. Differences in ocular pathology are noted. However, depletion of the $CD8^+$ T cells completely abolishes the efficacy, suggesting that in addition to antibody, $CD8^+$ T cells are a contributing factor in the control of virus spread and replication using the HSV-1 0ΔNLS vaccine in this unique model in which a significant proportion of $CD8^+$ T cells are committed to HSV gB specificity prior to immunization or exposure to HSV-1.

RESULTS

The HSV-1 0ΔNLS vaccine shows efficacy against ocular HSV-1 challenge in the absence of neutralizing antibody. Previously, we reported that the correlate of protection of the HSV-1 0ΔNLS-vaccinated mice was antibody (38). However, the absence of T cells was found to be necessary for the efficacy of the vaccine to maintain protection, presumably due to a lack of $CD4^+$ T cell support of the B cell response (40). To dissect the potential role of $CD8^+$ T cells in HSV-1 0ΔNLS vaccine efficacy, gBT-I.1 mice were chosen in which >85% of all T cell receptors on $CD8^+$ T cells are committed to the recognition of a single peptide found within HSV-1 gB (48). The results show that HSV-1 0ΔNLS vaccinated gBT-I.1 mice are more resistant to ocular challenge, with 24/27 HSV-1 0ΔNLS-vaccinated mice surviving acute infection compared to 8/19 control-vaccinated animals (Fig. 1A). This difference in survival was not reflected by antibody neutralization titers since only 3/17 HSV-1 0ΔNLS-vaccinated mice evaluated had measurable neutralization titers (58 ± 23) compared to 0/16 vehicle-vaccinated mice (Fig. 1B). Even in mice that survived ocular HSV-1 challenge, the neutralization antibody titer in the gBT-I.1-vaccinated groups was modest in comparison to surviving wild-type (WT) mice that range in antibody-neutralizing titer from 1,600 to 3,200 (Fig. 1C).

Since there was a decisive difference in survival in challenged gBT-I.1 mice that had been vaccinated with vehicle versus HSV-1 0ΔNLS, a likely explanation would include preventing virus replication. Whereas there was no detectable difference in viral titers recovered in the cornea comparing vehicle- to HSV-1 0ΔNLS-vaccinated mice (Fig. 2A), there was a significant reduction in infectious virus obtained from the TG (Fig. 2B) and brain stem (BS) (Fig. 2C) of HSV-1 0ΔNLS-vaccinated animals. Taken together, the results

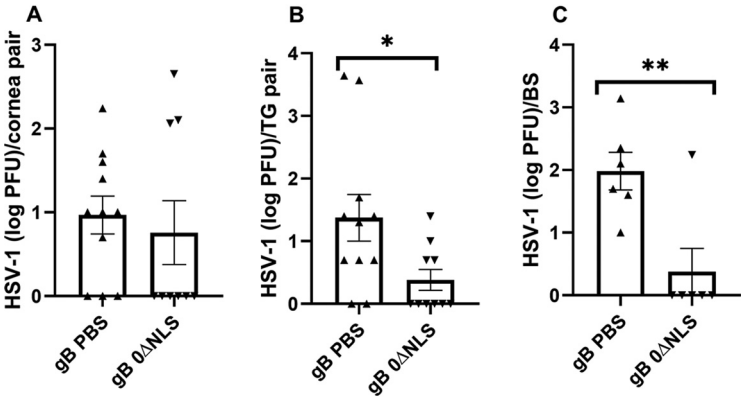

FIG 2 HSV-1 0ΔNLS vaccine suppresses viral titer in the TG but not cornea during acute infection. Vaccinated gBT-I.1 mice ($n = 6$ to 11/group) were infected with HSV-1 (10^4 PFU/cornea) 30 days post-boost. (A to C) Seven days p.i., the mice were exsanguinated, and the corneas (A), TG (B), and BS (C) were collected and assayed for viral titer by plaque assay. Data are presented as mean ± SEM taken from two to three experiments. *, $P < 0.05$; **, $P < 0.02$ comparing vehicle- to the 0ΔNLS-vaccinated group as determined by Mann-Whitney, two-tailed nonparametric test.

suggest that in the near absence of neutralizing antibody, HSV gB-specific $CD8^+$ T cells in gBT-I.1 transgenic mice contribute to the HSV-1 0ΔNLS vaccine efficacy against ocular challenge that closely aligns with preventing virus spread and/or replication in the TG and BS.

HSV-1 0ΔNLS-vaccinated mice show a reduction in corneal neovascularization but not opacity. Blood and lymphatic vessel genesis in the cornea have been reported to occur in response to HSV-1 infection (50–52). To determine whether HSV-1 0ΔNLS vaccination preempts corneal neovascularization in the gBT-I.1 transgenic mice, vaccinated animals were assessed for blood and lymphatic vessel growth into the cornea following HSV-1 infection. The results show that HSV-1 0ΔNLS-vaccinated gBT-I.1 mice display little corneal neovascularization compared to vehicle-vaccinated animals following challenge (Fig. 3A and B). The difference in response correlates with a loss of expression of vascular endothelial growth factor A (VEGF A) and interleukin-6 (IL-6) but not angiopoietin 2 (ANG-2) or fibroblast growth factor 2 (FGF-2) during the acute phase of infection (Fig. 3C).

In addition to corneal angiogenesis, opacity is another hallmark manifestation that is often associated with experimental herpes stromal keratitis (53, 54). Therefore, corneal opacity was evaluated in vaccinated gBT-I.1 transgenic mice following ocular challenge. Unlike differences observed in angiogenesis, HSV-1 0ΔNLS-vaccinated mice showed a similar degree of opacity as the vehicle-vaccinated group following infection, significantly above uninfected controls (Fig. 4). We interpret this result to suggest the HSV-1 0ΔNLS vaccine in gBT-I.1 transgenic mice does not fully compensate for the loss of antibody in terms of maintaining collagen architecture as is observed in wild-type mice (40). Since the gBT-I.1 transgenic mice lack a normal frequency of $CD4^+$ T cells and maintain precommitted $CD8^+$ T cells, factors in addition to antibody likely contribute to the preservation of collagen lamellae architecture post-HSV-1 infection in a more normal immunological setting.

Resistance to HSV-1 infection in the TG of HSV-1 0ΔNLS-vaccinated mice is reflected by functional activity. Leukocyte infiltration into the cornea and TG, a common response to ocular HSV-1 infection, is thought to contribute to tissue pathology (55–58). Therefore, immune cell infiltration was evaluated in the cornea during acute infection. The results show that within the cornea of gBT-I.1 transgenic mice during acute infection, there was no difference in the number of myeloid-derived cell ($CD45^+CD11b^+Ly6G/C^{+/-}$) or T lymphocyte ($CD45^+CD3^+CD4^+$ and $CD45^+CD3^+CD8^+$) populations, including HSV-1 gB-specific $CD8^+$ T cells (Fig. 5A). A similar finding was observed in the TG of vaccinated gBT-I.1 mice infected with HSV-1 (Fig. 5B).

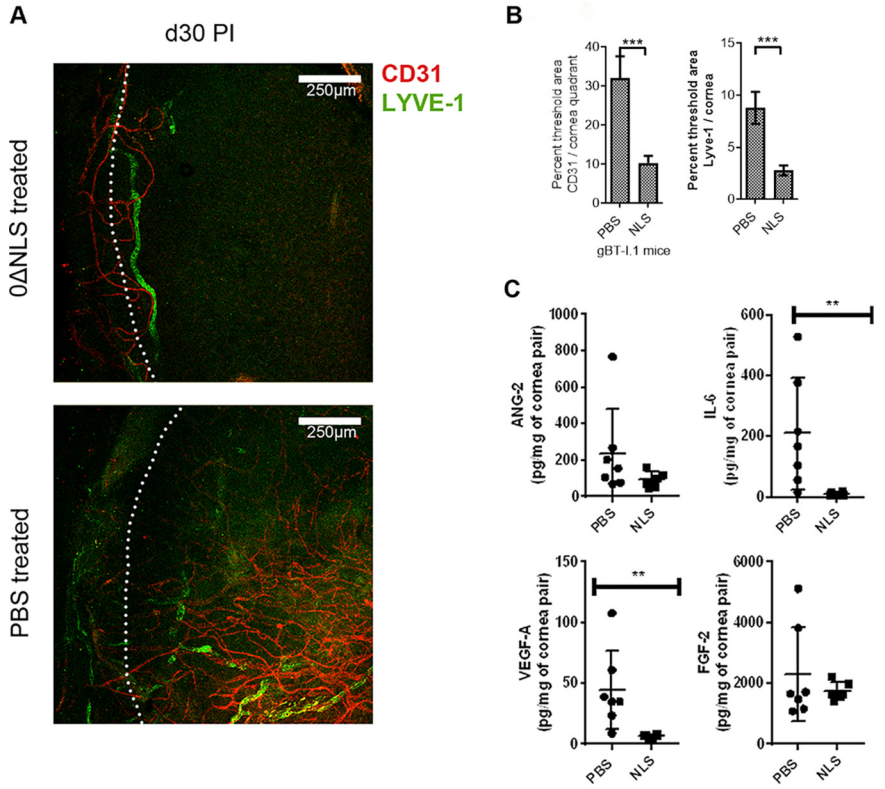

FIG 3 The HSV-1 0ΔNLS vaccine suppresses cornea neovascularization but not opacity. Vaccinated gBT-I.1 mice ($n = 4$ to 12 mice/group) were infected with HSV-1 (10^4 PFU/cornea) 30 days postboost. Thirty days p.i., surviving mice were exsanguinated, and corneas were removed and stained for blood (CD31, red) and lymphatic vessels (LYVE-1, green). (A) A representative image of cornea from an HSV-1 0ΔNLS-vaccinated mouse (0ΔNLS treated) and vehicle (PBS-treated) animal. (B) Summary analysis of the cornea area (excluding limbus, white dotted line in the images) occupied by blood and lymphatic vessels. ***, $P < 0.001$ comparing vehicle (PBS)- to HSV-1 0ΔNLS-vaccinated groups as determined by Mann-Whitney U rank test. (C) Vaccinated gBT-I.1 mice ($n = 6$ to 7 mice/group) infected with HSV-1 (10^4 PFU/cornea) 30 days postboost. The mice were exsanguinated 7 days p.i. The corneas were processed and analyzed for analyte content, including angiopoietin-2 (Ang-2), IL-6, vascular endothelial growth factor (VEGF) A, and fibroblast growth factor (FGF) 2 by suspension array. Data are presented as mean ± SEM. **, $P < 0.01$ comparing vehicle (PBS)- to HSV-1 0ΔNLS (NLS)-vaccinated groups by Mann-Whitney rank order test.

Since $CD8^+$ T cell function has previously been reported to be altered in the TG following HSV-1 infection in C57BL/6 mice (59), and a polyfunctional effector $CD8^+$ T cell response has been associated with greater surveillance against HSV-1 in patients (60, 61), the functional response of $CD8^+$ T cells from the TG of vaccinated gBT-I.1 mice was evaluated post-HSV-1 infection. Initially, gates were established for the expression of each molecule under evaluation comparing stimulated with nonstimulated cells (Fig. 6). Analysis of cells for IFN-γ, granzyme B (62), and CD107a (63) expression following *in vitro* gB peptide stimulation were then collated using SPICE software (Fig. 7). The pie charts represent the average frequencies of stimulated $CD8^+$ T cells, with each segment of the chart denoting every possible combination of the three functional molecules analyzed (Fig. 7A). Of note, the frequency of $CD8^+$ T cells obtained from the TG of HSV-1 0ΔNLS-vaccinated gBT-I.1 mice post-gB peptide stimulation expressing IFN-γ, granzyme B, and CD107a was significantly elevated compared to $CD8^+$ T cells from the phosphate-buffered saline (PBS)-vaccinated group (Fig. 7B). This group made up the majority of the $CD8^+$ T cell profile from either group of vaccinated mice. In contrast, the frequency of $CD8^+$ T cells expressing either CD107a or granzyme B from PBS-vaccinated gBT-I.1 mice was significantly elevated above that by $CD8^+$ T cells from the 0ΔNLS-vaccinated animals (Fig. 7B). The frequency of any combination of dual-expressing effector $CD8^+$ T cells was <2% and was not different comparing the two

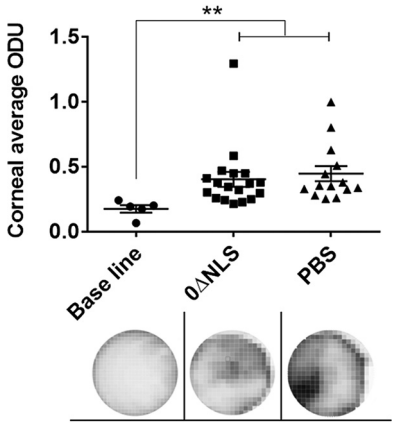

FIG 4 HSV-1 0ΔNLS-vaccinated mice display similar corneal opacity as the vehicle-vaccinated group post-HSV-1 infection. gBT-I.1 mice were vaccinated and subsequently infected as described in Materials and Methods. Seven days p.i., the mice were exsanguinated, and the corneas were removed. The upper panel is the summary of corneal opacity measured at the optical density (light scattering) of 500 nm wavelength in a 30 by 30 matrix distributed over the corneal surface. The average value of the aforementioned matrix per cornea was graphed. The results are expressed in optical density units (ODU). The baseline was made with mice scratched in the cornea but not infected with HSV-1. The lower panel is a representative image at ×32 magnification of three corneas from scarified, uninfected (baseline, $n = 3$), HSV-1 0ΔNLS (0ΔNLS, $n = 9$)-, and vehicle (PBS, $n = 7$)-vaccinated mice on day 7 p.i. **, $P = 0.0019$ comparing the vaccinated, infected mice to the uninfected control group as determined by the nonparametric Kruskal-Wallis ANOVA.

groups of vaccinated mice. In addition, it is noteworthy that the frequency of $CD8^+$ T cells that did not express any of these functional markers was significantly elevated in the PBS-vaccinated group compared to the 0ΔNLS-vaccinated mice, indicating a higher degree of unresponsiveness to gB peptide stimulus in the PBS-vaccinated gBT-I.1 transgenic animals (Fig. 7B). Consistent with these findings, the individual number of IFN-γ-secreting $CD8^+$ T cells obtained from the TG of HSV-1 0ΔNLS-vaccinated mice in response to $gB_{495–505}$ peptide was also greater than the vehicle-vaccinated control. Specifically, vehicle-vaccinated mice retained 73 ± 10 IFN-γ-secreting $CD8^+$ T cells within the TG compared to 132 ± 15 from HSV-1 0ΔNLS-vaccinated mice as measured

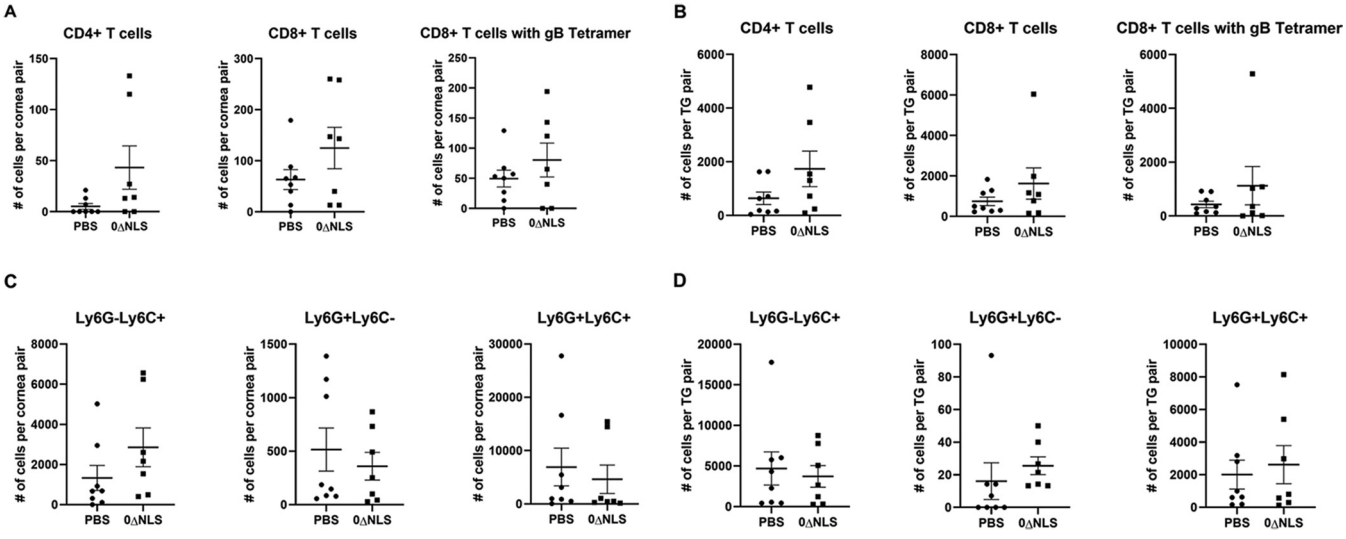

FIG 5 Leukocyte content in the corneas and TG of vaccinated gBT-I.1 mice day 7 postinfection. Mice were vaccinated with vehicle (PBS) or HSV-1 0ΔNLS (NLS) and infected with HSV-1 as described in Materials and Methods. (A and B) At day 7 p.i., the corneas (A) and TG (B) were excised and analyzed by flow cytometry for $CD3^+CD4^+$ T cells, $CD3^+CD8^+$ T cells, $CD3^+CD8^+$HSV $gB_{405-505}$ tetramer$^+$, and (C) corneas and (D) TG for $CD45^+CD11b^+Ly6G^+Ly6C^-$ cells ($CD11b^+Ly6G^+$ neutrophils), $CD45^+CD11b^+Ly6G$-$Ly6C^+$ cells ($CD11b^+Ly6C^+$ macrophage), and $CD45^+CD11b^+Ly6G^+Ly6C^+$ cells ($CD11b^+Ly6G^+Ly6C^+$ cell inflammatory macrophage). Data are presented as means ± SEM; $n = 7$ to 8 mice/group.

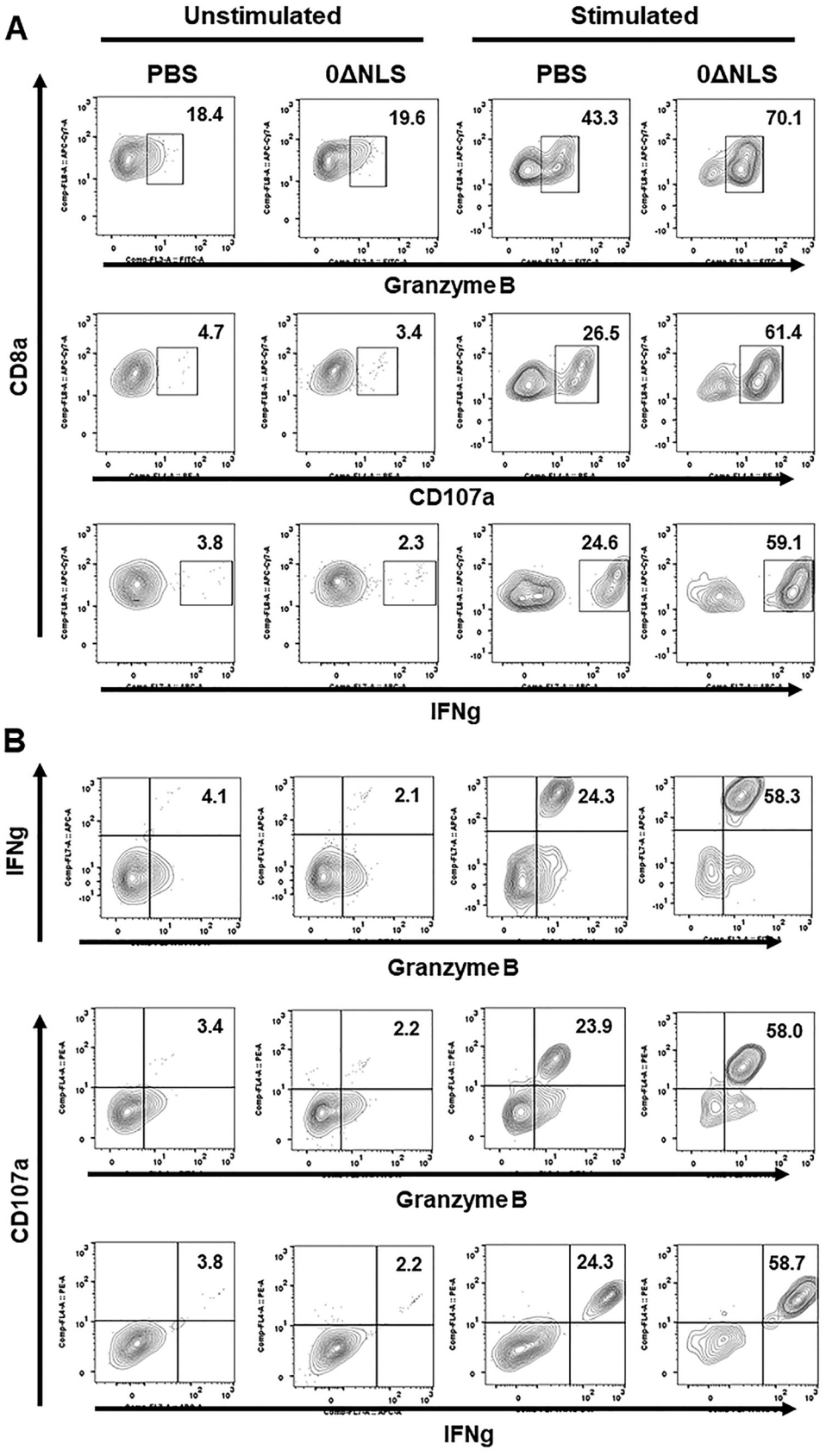

FIG 6 Stimulation of CD8 T cells from trigeminal ganglia (TG) results in amplification of expression of IFN-γ, CD107a, and granzyme B. TG harvested from vehicle (PBS)- or HSV-1 virus 0ΔNLS-vaccinated mice 7 days

(Continued on next page)

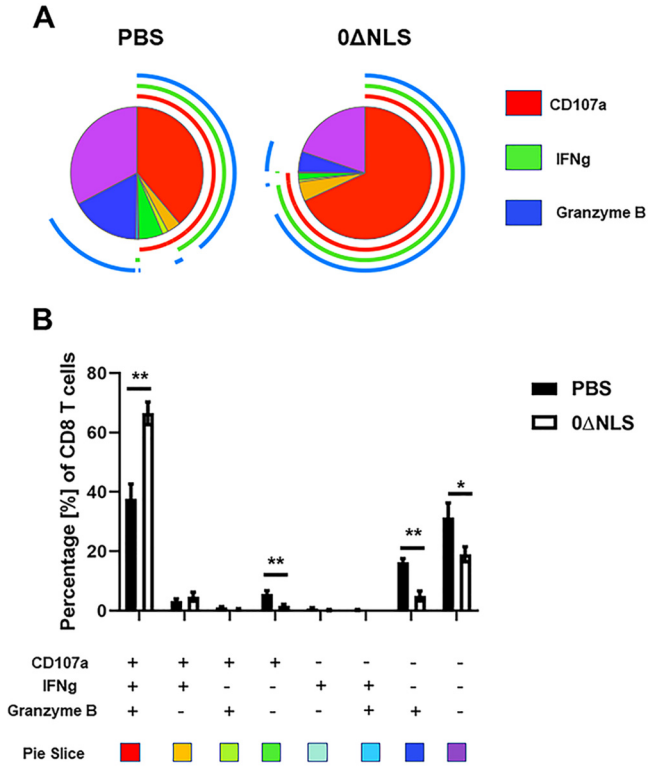

FIG 7 CD8 T cells from trigeminal ganglia of 0ΔNLS-vaccinated mice display a significantly higher polyfunctional effector frequency compared to PBS-vaccinated mice. The trigeminal ganglia from vaccinated mice ($n = 5$/group) infected with HSV-1 7 days previously were harvested and manually homogenized, and single cell suspensions were stimulated with HSV-1 gB peptide followed by $CD8^+$ T cell staining for CD107a, IFN-γ, and granzyme B expression as described in Materials and Methods. Stained cells were analyzed by flow cytometry, and the frequency of $CD8^+$ T cells expressing CD107a, IFN-γ, and granzyme B was determined using FlowJo software. The polyfunctional profile of the effector cells was analyzed with SPICE software and presented as pie charts. (A) The pie charts display the average frequency of $CD8^+$ T cells expressing any combination of CD107a, IFN-γ, and granzyme B from vaccinated mice. The inner segments show cells producing different combinations of analyzed analytes (listed in panel B, below the graph) and are color coded. The outer arcs around the circle indicate the frequency of cells producing one of the analyzed analytes (CD107a, IFN-γ, or granzyme B) and are color coded. The polyfunctional profile is determined by extension of the arcs that surround the pie chart. (B) Summary data presenting frequency of $CD8^+$ T cells producing different combinations of CD107a, IFN-γ, and granzyme B. The values are presented as the means ± SEM. **, $P < 0.01$; *, $P < 0.05$ as determined by Student's *t* test.

by enzyme-linked immunosorbent spot (ELiSPOT) assay ($P < 0.01$, $n = 6$ to 7/group as determined by Student's *t* test).

Therefore, in terms of functional markers displayed by $CD8^+$ effector T cells from the TG, more cells from the HSV-1 0ΔNLS-vaccinated mice expressed IFN-γ, CD107a, and granzyme B compared to the cells from the vehicle-vaccinated counterparts post-gB peptide stimulation.

We previously found that functional loss of effector cells correlates with the expression of exhaustion markers displayed by effector T cells in HSV-1-infected mice (64).

FIG 6 Legend (Continued)
postinfection were manually homogenized to generate single cell suspensions and stimulated with 10 μg/ml of HSV-1 gB (SSIEFARL) or left unstimulated for 24 h. CD107a Ab was added for the last 6 h of cell incubation followed by brefeldin A (GolgiPlug). Subsequently, the cells were stained with cell surface antigens (CD45, CD3, and CD8), fixed, and permeabilized, and following the permeabilization step were stained using anti-mouse IFN-γ, and anti-mouse/human granzyme B antibodies. (A) Frequency of CD8 T cells expressing CD107a, IFN-γ, or granzyme B, each presented individually in unstimulated and stimulated settings. (B) The frequency of CD8 T cells coexpressing two of three markers simultaneously. Each figure is representative of results from two independent experiments.

Therefore, analysis of exhaustion markers as well as the proliferation marker, Ki67 (65), was determined on the gB-specific CD8$^+$ T cells from the TG of vaccinated mice post-HSV-1 infection. Whereas there was no difference in overall proliferation by the effector CD8$^+$ T cells from PBS-vaccinated (42.2 $\pm$ 9.9%) versus 0ΔNLS-vaccinated (42.5 $\pm$ 8.7%) mice post-gB peptide stimulation, a greater number of CD8$^+$ T cells from the vehicle-vaccinated mice expressed significantly more lymphocyte activation gene 3 (LAG-3), programmed cell death 1 (PD-1), and T cell immunoglobulin and mucin domain-containing protein 3 (TIM-3) than cells from the TG of HSV-1 0ΔNLS-vaccinated mice 7 days postinfection (p.i.) (Fig. 8A and B). By comparison, PD-1 and TIM-3 but not LAG-3 expression was elevated on CD8$^+$ T cells from the cornea of PBS-vaccinated mice in comparison to cells from the 0ΔNLS-vaccianted animals 7 days p.i. (Fig. 9A and B). These results suggest cells from HSV-1 0ΔNLS-vaccinated animals are maintained at a higher functional level that coincides with a reduction in virus replication within the TG environment in this unique transgenic mouse model.

HSV-1 gB-specific CD8$^+$ T cells from HSV-1 0ΔNLS-vaccinated gBT-I.1 transgenic mice maintain an elevated metabolic level compared to cells from vehicle-vaccinated animals. T cell activation and function are intrinsically related to cellular metabolism, including glucose uptake and utilization (66, 67). Since the CD8$^+$ effector T cells from the HSV-1 0ΔNLS-vaccinated gBT-I.1 mice displayed an elevated polyfunctional phenotype compared to the effector T cells from vehicle-vaccinated mice p.i., the metabolic profile of these effector cells was examined. CD8$^+$ effector T cells from the HSV-1 0ΔNLS-vaccinated mice stimulated with $gB_{495–505}$ peptide displayed a higher basal rate of mitochondrial oxygen consumption (Fig. 10A and B) and extracellular acidification rate showing an increase in aerobic glycolysis and glycolytic capacity compared to $gB_{495–505}$ peptide-stimulated cells from vehicle-vaccinated mice (Fig. 10C and D). These results are consistent with an increase in effector function in terms of IFN-γ expression post-antigen stimulus by the gB-specific CD8$^+$ T cells from the 0ΔNLS-vaccinated mice, reinforcing the importance of glycolytic metabolism and effector T cell activity (68). Whether this observation holds true under normal circumstances (i.e., in the absence of a skewed preexisting population of $gB_{495–505}$-specific CD8$^+$ T cells) by effector CD8$^+$ T cells in response to additional HSV-1 peptide candidates requires further investigation.

Depletion of CD8$^+$ T cells in HSV-1 0ΔNLS-vaccinated gBT-I.1 mice renders mice highly susceptible to HSV-1 challenge. Thus far, HSV-1 0ΔNLS-vaccinated gBT-I.1 mice have been found to be resistant to challenge with HSV-1 as measured by survival, virus replication in the TG, and corneal neovascularization. To further demonstrate the contribution of these cells, vaccinated gBT-I.1 mice were depleted of CD8$^+$ T cells to determine if the absence of CD8$^+$ T cells increased susceptibility to HSV-1 infection. The results show CD8$^+$ T cell-depleted, HSV-1 0ΔNLS-vaccinated mice are highly sensitive to HSV-1 infection with a significant loss in survival and, inversely, an increase in infectious virus recovered from the TG during acute infection compared to isotypic IgG-control-treated, HSV-1 0ΔNLS-vaccinated mice (Fig. 11A and B). However, there was no difference in viral content recovered in the cornea (Fig. 11C) or shed in the tear film (Fig. 11D) during acute infection. These results suggest CD8$^+$ T cells participate in surveillance of HSV-1 in the TG but not the cornea of vaccinated mice in which the majority of CD8$^+$ T cells are precommitted to $gB_{495–505}$ specificity.

DISCUSSION

Strategies to develop vaccines against HSV-1 and -2 have been discussed and reviewed for some time (69). In 2000, it was predicted it would take 7 years at a cost of $240 million to generate a licensed vaccine against HSV (70). To date, there are no ongoing clinical trials to assess vaccine candidates to prevent primary HSV-1 infection or block HSV-1 reactivation. However, there are novel experimental approaches that seem to suggest specific virus-encoded proteins may be candidates as immunogens to generate protective antibody and cytotoxic T cell responses to block acute virus infection or reactivation. Specifically, using computational algorithms to screen HLA-

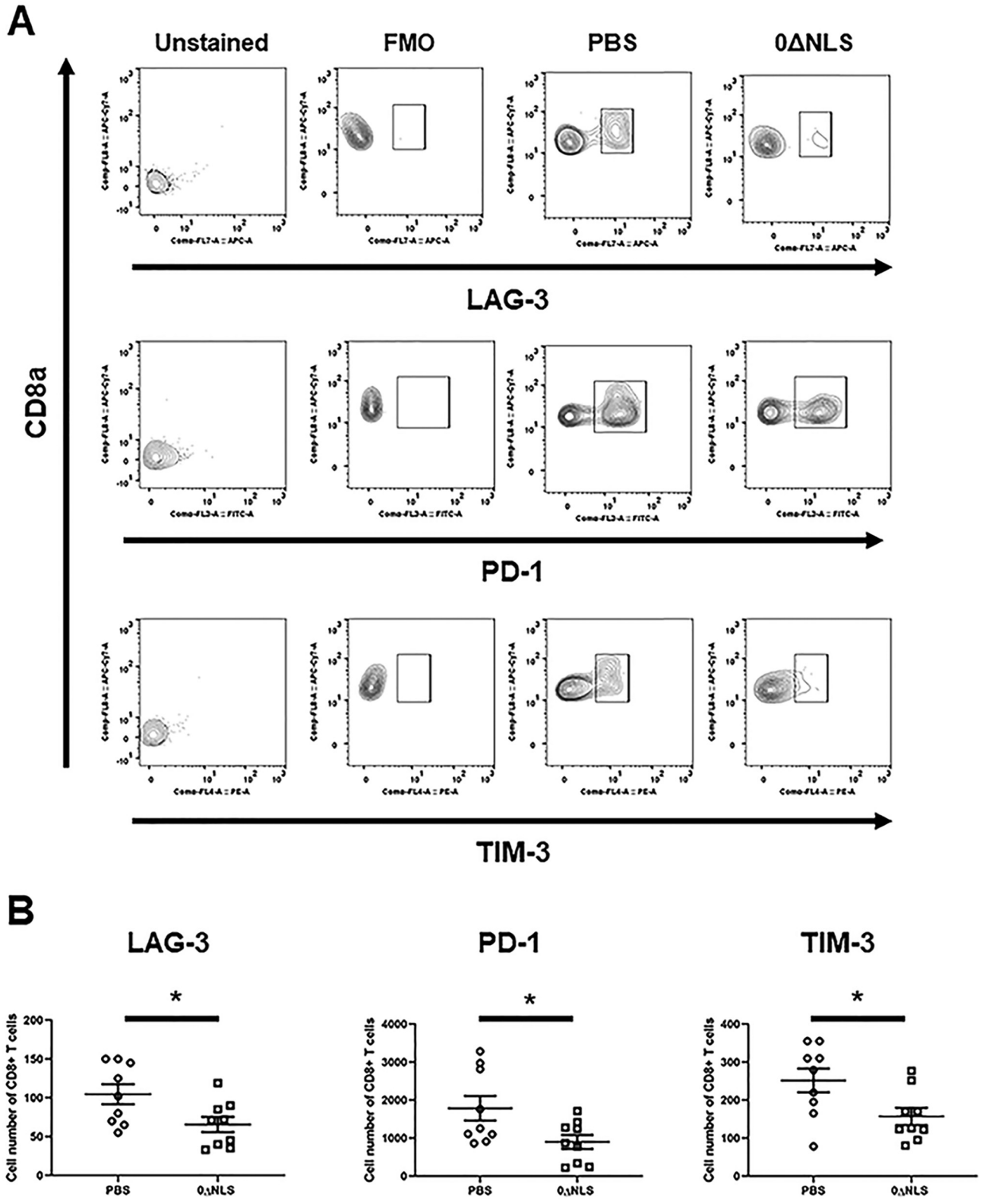

FIG 8 Functional markers expressed by CD8$^+$ effector T cells from the TG of HSV-1 0ΔNLS-vaccinated gBT-I.1 mice are elevated compared to CD8$^+$ effector T cells from vehicle-vaccinated animals. Single cell suspensions from TG harvested 7 days p.i. Cells were stained with an antibody panel set targeting CD45, CD3, and CD8 cells along with exhaustion markers (LAG-3, PD-1, or TIM-3). (A) A representative gating profile of stained CD8$^+$ T cells for LAG-3, PD-1, and TIM-3 from mice vaccinated with PBS or 0ΔNLS along with the fluorescence minus one (FMO) and unstained controls is shown. (B) The number of CD8$^+$ T cells expressing LAG-3, PD-1, or TIM-3 from mice vaccinated with PBS or 0ΔNLS is shown. The data set is a summary of three independent experiments expressed as means ± SEM. *, $P < 0.05$ as determined by Student's test comparing PBS- to 0ΔNLS-vaccinated mice; $n = 9$/group.

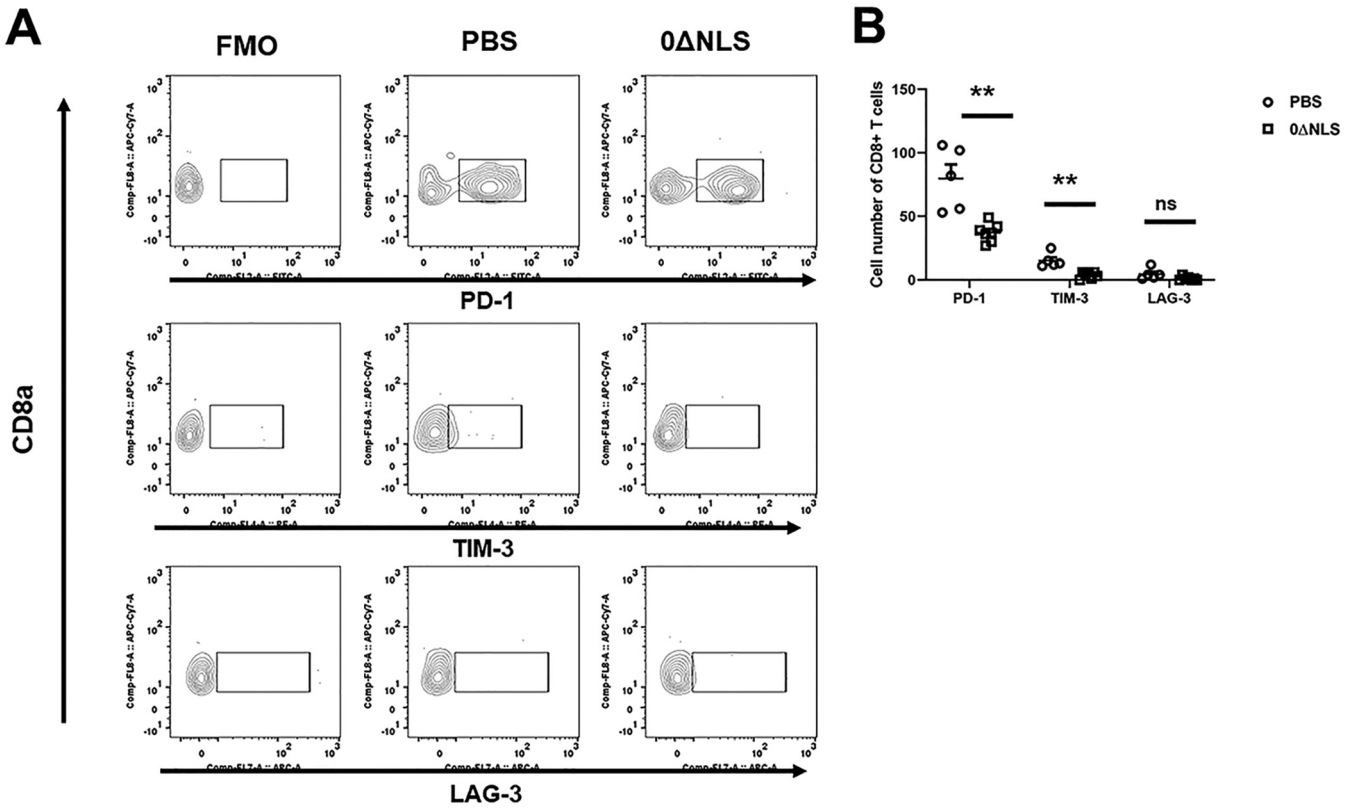

FIG 9 CD8 T cells in the cornea of vaccinated mice show reduced numbers of cells expressing PD-1 and TIM-3 in comparison to vehicle-treated mice postinfection. Corneas were harvested from vaccinated mice 7 days postinfection. Following processing, the cells were stained with an antibody panel for CD45, CD3, and CD8 along with the exhaustion markers Lag-3, PD-1, and Tim-3. (A) A representative gating strategy of stained $CD8^+$ T cells for LAG-3, PD-1, and TIM-3 from mice vaccinated with PBS or 0ΔNLS along with the FMO is included. (B) The number of $CD8^+$ T cells expressing LAG-3, PD-1, or TIM-3 from mice vaccinated with PBS ($n = 5$) or 0ΔNLS ($n = 7$) is shown. The data are a summary of two independent experiments expressed as means ± SEM. **, $P < 0.01$, as determined by Student's *t* test comparing $CD8^+$ T cells from PBS- to those from 0ΔNLS-vaccinated mice; ns, not significant.

A*02:01 viral protein binding regions, one group has identified several epitopes that are recognized by human HLA-A*A2:01-restricted $CD8^+$ cytotoxic T cells from HSV-1-seropostive patients that are asymptomatic for infection (71–74). Using HLA-A*02:01-restricted transgenic rabbits and mice (75, 76), this group identified HLA-A*02:01-restricted viral peptides used as $CD8^+$ T cell-based vaccines that were found to protect vaccinated animals against ocular HSV-1 infection (71–74). Another group has found that monoclonal antibodies derived from B lymphocytes of patients vaccinated with a bivalent recombinant HIV gp120 containing the herpesvirus entry mediator (HVEM) binding domain of glycoprotein D (gD) protect mice from ocular HSV-1 infection (77). While these findings show significant promise, both groups mentioned above use subjective measurements to show that these vaccines or antibodies administered to mice protect against corneal pathology, consistent with most publications in the field. However, we would submit that a more quantitative means to measure ocular pathology and function is necessary to truly evaluate the efficacy of a vaccine against experimental ocular HSV-1 infection, including neovascularization (52, 78), corneal denervation (79, 80), inflammatory hypoxia (81), opacity (82), and visual acuity (40). To date, the HSV-1 0ΔNLS vaccine is the only vaccine to have demonstrated prophylactic efficacy against ocular HSV-1 challenge in not only establishing sterile immunity and significant reduction in the establishment of a latent infection but also preventing corneal pathology and preserving the visual axis (40). It is notable that many of the HSV-1-encoded proteins identified to possess protective epitopes used as vaccines against HSV-1 infection (71–74) are recognized by the HSV-1 0ΔNLS vaccine (40), suggesting that a cocktail approach is the most likely path to a truly effective vaccine other than live-attenuated virus candidates.

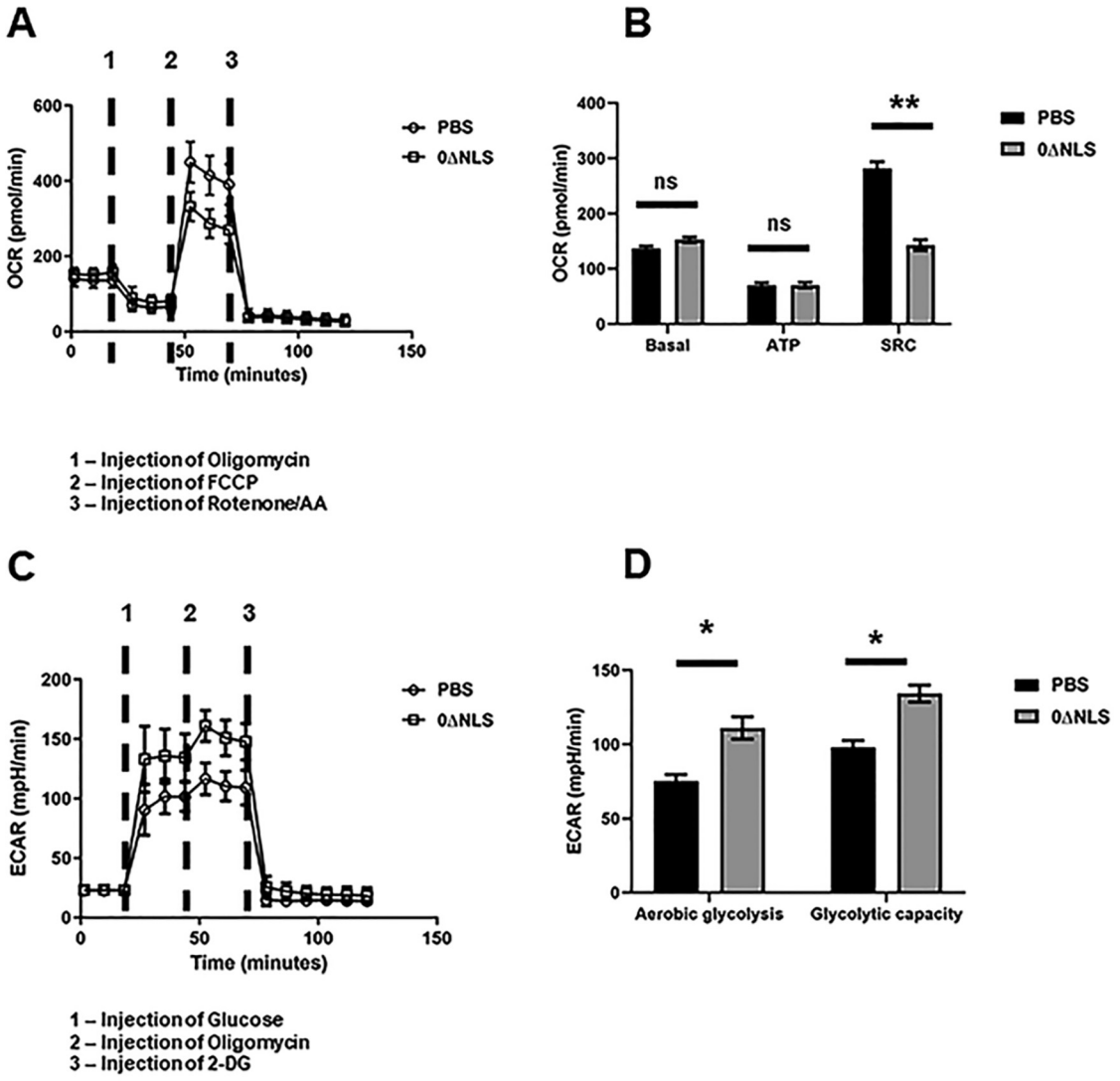

FIG 10 HSV-1 gB-specific CD8$^+$ T cells from HSV-1 0ΔNLS-vaccinated gBT-I.1 mice display elevated metabolic demand poststimulation compared to cells from vehicle-vaccinated mice. gBT-I.1 T cell receptor (TCR) transgenic mice were vaccinated and 3 weeks later boosted with vehicle (PBS, $n = 6$) or 10^5 PFU HSV-1 0ΔNLS ($n = 5$). Thirty days postboost, the mice were infected with HSV-1 (10,000 PFU/eye), and 7 days p.i., mandibular lymph nodes were harvested, and isolated T cells were stimulated with gB peptide (10 μg/ml) followed by analysis of key parameters of mitochondrial function, including the oxygen consumption rate (OCR) as well as glucose consumption (glycolysis stress test) 48 h poststimulation. (A) The metabolic flux measured at the baseline and after injection of oligomycin, FCCP, and rotenone/antimycin (Rot/AA) presented as the mean ± SD. (B) The summary of the metabolic parameters under analysis (basal respiration, ATP production, and spare respiratory capacity or SRC) presented as the mean ± SEM. (C) The metabolic flux measured at the baseline and after injection of glucose, oligomycin, and 2-deoxy-glucose (2-DG) presented as the mean ± SD. (D) The summary for aerobic glycolysis and glycolytic capacity presented as the mean ± SEM. **, $P < 0.01$; *, $P < 0.05$; ns, not significant as determined by Student's *t* test.

Experimentally, antibodies have long been appreciated as a means to protect the host against ocular HSV-1 infection (83, 84). The current study was undertaken to determine if the HSV-1 0ΔNLS vaccine retained efficacy against ocular HSV-1 infection in the absence of neutralizing antibody in mice that have an exaggerated precommitted population of CD8$^+$ T cells specific for a single HSV antigenic epitope, $gB_{495-505}$. The lack of a measurable neutralizing antibody titer in gBT-I.1 transgenic compared to WT vaccinated mice may, in part, be due to the modest number of CD4$^+$ T cells that reside in the organized lymphoid tissue, including the mandibular lymph node post-HSV-1 infection that could contribute to facilitating the humoral immune process (85). Previously, we reported that gBT-I.1 mice were more resistant to HSV-1 infection compared to wild-type mice measured by reduced infectious virus recovered in the

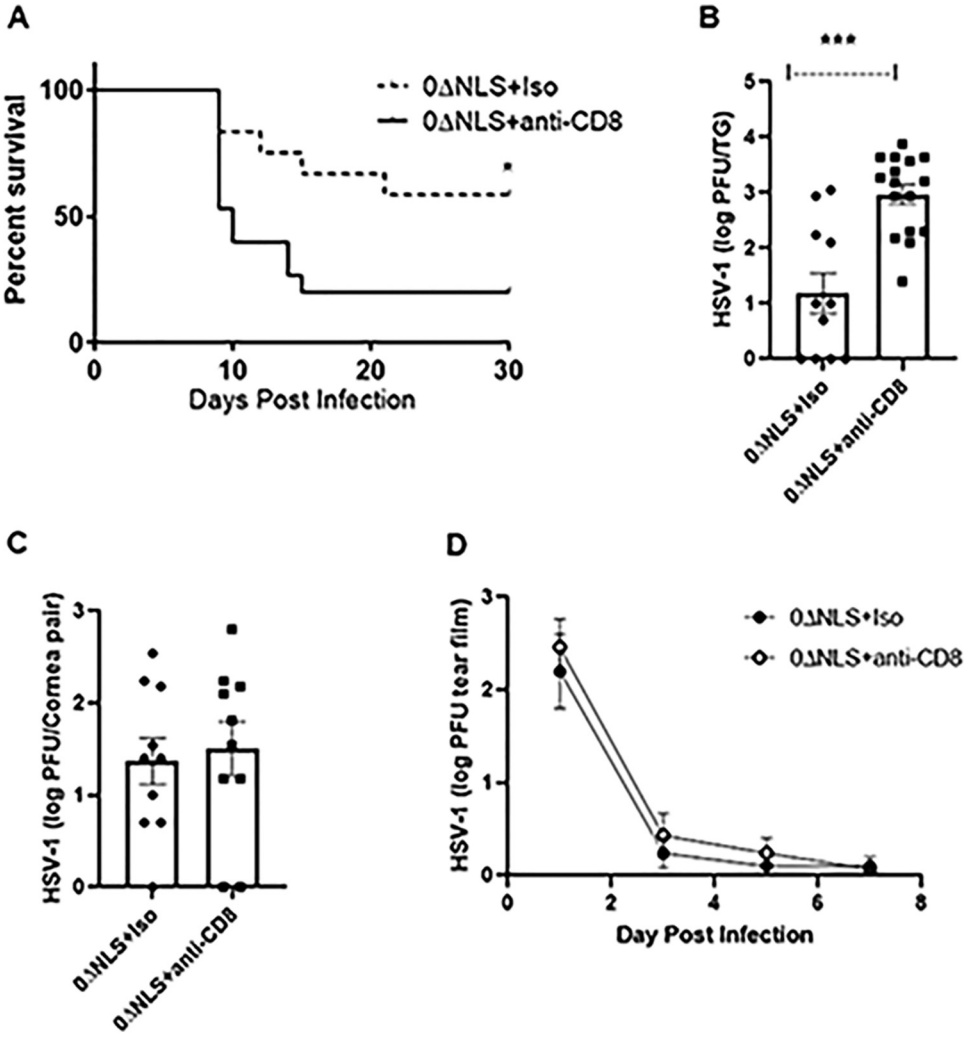

FIG 11 Depletion of CD8$^+$ T cells renders HSV-1 0ΔNLS-vaccinated mice susceptible to virus challenge. Male and female gBT-I.1 mice were vaccinated and boosted with vehicle or HSV-1 0ΔNLS. Vaccinated mice were treated and infected with 10^5 PFU HSV-1 as described in Materials and Methods. (A) Mice ($n = 12$ to 16/group) were monitored for survival over 30 days. *, $P < 0.05$ comparing the two groups as determined by the Mantel-Cox test. (B and C) Mice treated as described above were euthanized 7 days postinfection, and the TG (B) and corneas (C) were removed and processed for viral titer by plaque assay. Data are expressed as mean ± SEM; $n = 10$ to 16/group. ***, $P < 0.001$ comparing the two groups as determined by Student's t test. (D) Vaccinated mice ($n = 7$ to 9/group) treated as described above were monitored for shed HSV-1 in the tear film from day 1 to day 7 postinfection. Each point represents the mean ± SEM.

cornea during acute infection and significantly less corneal blood vessel genesis by day 30 p.i. (85). The present study demonstrates the susceptibility of the gBT-I.1 transgenic mice in terms of corneal pathology to a substantially higher infectious dose of virus, 10 to 100 times higher than that previously reported (85). The angiogenic response displayed by the vehicle-vaccinated gBT-I.1 mice correlated with an increase in VEGF-A and IL-6, two proangiogenic factors that have been associated with HSV-1-induced corneal neovascularization (86, 87). The HSV-1 0ΔNLS vaccine was found to block corneal neovascularization but had no impact on the ocular viral load, suggesting virus alone does not drive neovascularization, consistent with a previous report (88).

The impact of the HSV-1 0ΔNLS vaccine on virus replication was observed in the TG of the vaccinated gBT-I.1 mice in which viral loads were reduced 10-fold. This enhanced capacity to block virus replication was associated with an increase in IFN-γ-producing HSV-1 gB-specific CD8$^+$ T cells that reside in the tissue. IFN-γ has been described as a potent anti-HSV-1 cytokine that suppresses virus replication during acute infection and

reactivation during latency (89–92). Of note, the enhanced IFN-γ, CD107a, and granzyme B expression by the antigen-stimulated $CD8^+$ T effector cells was inversely correlated with the T cell checkpoint receptors PD-1, LAG-3, and TIM-3, consistent with the inhibitory capacity of these molecules on $CD8^+$ T cell function (93–95). Coupled with this finding, a previous study found that blocking expression of these inhibitory coreceptors increased the frequency of polyfunctional $CD8^+$ effector T cells and suppressed viral loads in HSV-1-infected, humanized transgenic rabbits (96). However, in that study, it was also reported that treatment of animals with antibodies targeting the inhibitory coreceptors was found to increase proliferation as measured by Ki67 staining, whereas in the present study, there was no difference in expansion of the effector $CD8^+$ T cell population comparing vehicle- to HSV-1 0ΔNLS-vaccinated mice. Thus, in the gBT-I.1 transgenic mouse model, it would appear that the HSV-1 gB-specific $CD8^+$ T cells of HSV-1 0ΔNLS-immunized animals are more resilient to environments that influence the functional nature of effector T cells during acute HSV-1 infection such as that found in the TG as opposed to only proliferation. A caveat to this conclusion is that a single time point was chosen to evaluate the T cell response and the skewed gB-specific nature of the $CD8^+$ T cells. Whether the vaccine impacts the magnitude or timing of the response by the effector $CD8^+$ T cells at earlier time points has not been measured in this study.

In this model, the principal driver of protection is the gB-specific $CD8^+$ T cell, as depletion of this population adversely affects the outcome of mice in terms of survival and virus replication. This result is not unexpected since the majority of T cells in these transgenic mice are specific for the $gB_{495–505}$ peptide. Glycoprotein B is an essential component in the fusion process of the pathogen's entry into the host cell and cell-to-cell spread (97, 98). Other groups have used this protein, gB peptides, or antibodies directed against specific regions of the protein to demonstrate that vaccination or passive immunization is highly effective in reducing anterograde transport of HSV-1 or virus-induced mortality following challenge (60, 99, 100). While we believe gB or gB-derived peptides alone in the form of a vaccine with adjuvants are not sufficient to provide broad protection against HSV-1 infection especially as it relates to preserving the visual axis, we would submit that the inclusion of gB or gB peptides should be considered a necessary component of a highly effective viral protein vaccine cocktail developed against HSV-1 infection. As the HSV-1 0ΔNLS vaccine-generated antiserum recognizes gB along with several other structural or nonstructural virus-encoded proteins and is shown to maintain the visual axis with minimal tissue pathology (40), our previous study supports the concept that single subunits alone will likely fail. Thus, we submit that a successful vaccine will incorporate several components of the viral antigen repertoire, including tegument and capsid proteins, glycoproteins, and nonstructural, primarily intracellular proteins along with an effective adjuvant to elicit humoral (antibody) and cell-mediated responses to protect against initial exposure or virus reactivation as experimental findings suggest (40, 74).

MATERIALS AND METHODS

Mice and virus. Male and female C57BL/6 (WT) mice (8 to 12 weeks of age; The Jackson Laboratory, Bar Harbor, ME) and HSV-1 gBT-I.1 T cell receptor transgenic mice (48) on a WT background were maintained in a specific-pathogen-free animal facility at the Dean McGee Eye Institute. These mice possess 20- to 30-fold more HSV gB-specific $CD8^+$ T cells in the draining lymph nodes compared to their WT counterparts with significantly fewer total $CD4^+$ T cells 7 days post-ocular HSV-1 infection. The offspring of gBT-I.1 breeders were genotypically validated prior to use in experiments. This study was approved by the Oklahoma University Health Sciences Center (OUHSC) animal care and use committee (protocol numbers 16-087 and 19-060) and performed in adherence to the National Institutes of Health *Guide for the Care and Use of Laboratory Animals*. HSV-1 (strain McKrae) was propagated in green monkey kidney cells (Vero cells; ATCC), and the stock (1×10^9 PFU/ml) was aliquoted and stored at −80°C until single use.

HSV-1 infection. Mice were anesthetized for all procedures by intraperitoneal (i.p.) injection of ketamine (100 mg/kg body weight) plus xylazine (5.0 mg/kg) and were euthanized by cardiac perfusion of 10 ml PBS for tissue collection. Animals (8 to 12 weeks old) were vaccinated with HSV-1 0ΔNLS (10^5 PFU) using a prime/boost approach via ipsilateral footpad (subcutaneous) and quadriceps (intramuscular) injection 3 weeks later as previously described (38). PBS alone served as the vehicle control. Thirty days following the

secondary boost, anesthetized mice were infected with 1×10^4 – 1×10^5 PFU HSV-1 McKrae to each cornea following partial epithelial debridement with a 25-gauge needle in a 3-μl volume PBS.

Viral titer. Following corneal infection, mice were euthanized at day 7 postinfection (p.i.), and the corneas, trigeminal ganglia (TG), and brain stems (BS) were collected and frozen at −80°C until plaque assays were performed as previously described (101).

Flow cytometry. Corneas, TG, and mandibular lymph nodes (MLNs) were collected at day 7 p.i. The extracted corneas were exposed to Liberase TL (Roche) for 30 min at 37°C. Digested tissue was filtered through a 40-μm cell strainer and washed with staining buffer (PBS supplemented with 2% fetal bovine serum [FBS]). TG were homogenized in a Dounce homogenizer for 30 strokes in RPMI 1640 medium containing 10% FBS and antimycotic/antibiotic solution (complete medium). The resulting suspension was filtered through a 40-μm mesh, centrifuged at 300 $\times$ *g* for 5 min, and decanted, and the pellet was resuspended in 2.0 ml of complete medium. MLNs were macerated into a single cell suspension in 3.5 ml of complete medium. One hundred microliters of single cell suspensions was then incubated in 1 to 2 μl Fc block CD16/CD32 (Thermo Fisher Scientific, Waltham, MA) diluted in 1% bovine serum albumin (BSA) in 1$\times$ PBS for 15 min and labeled with a combination of 1 μl each of CD45 efluor450, CD19 PE, B220 APC-Cy7, EpCAM efluor450, CD4 APC-Cy7, CD8 PE, CD11b FITC and PE-Cy7, Ly6-G APC, Ly6-C PE, and CD11c PE-Cy7 (Thermo Fischer Scientific) diluted in 1% BSA in 1$\times$ PBS for 30 min. In the case of tetramer staining, cells were labeled with a combination of CD3 PE-Cy7, CD8-APC-Cy7, and gB-PE. Cells were then washed twice by adding 1 ml of 1% BSA in 1$\times$ PBS, centrifuging for 5 min at 300 $\times$ *g*, and decanting the supernatant. Cells were then fixed in 1 ml of 1% paraformaldehyde overnight and resuspended in 1 ml of 1% BSA in 1$\times$ PBS to be analyzed on a MacsQuant 196 flow cytometer (Miltenyi Biotech). Gating strategies were identical to those previously described (102).

To evaluate expression of exhaustion markers within CD8 T cells, the cornea and TG single cell suspensions were stained with CD45-Pacific blue, CD8-APC-Cy7, CD3-PECy7, CD279 (PD-1)-FITC, CD366 (TIM-3)-PE, and CD223 (LAG-3)-APC (all BioLegend) and incubated 30 min on ice. Next, the stained cells were washed with staining buffer (PBS supplemented with 1% BSA) and fixed with 2% paraformaldehyde and acquired on flow cytometry within 48 h.

To determine the function and proliferation cell rate of $CD8^+$ T cells, CD107a, granzyme B, and IFN-γ expression within CD8 T cells was evaluated. TG single cell suspensions were *ex vivo* stimulated with 10 μg/ml $gB_{495-505}$ peptide (SSIEFARL) in 4 ml of RPMI 1640 medium containing 10% FBS in 10 ml snap-capped tubes (Fisher) for 24 h in the incubator at 37°C, and 5% CO_2 (one TG single cell suspension/tube). For the last 6 h of cell stimulation, CD107a-PE Ab was added directly to the cell culture followed by brefeldin A (GolgiPlug). After the incubation, the cells were washed with PBS (supplemented with 5% PBS and 0.09% NaN_3) and stained with antibodies (Abs) targeting CD8 T cells ($CD45^+CD3^+CD8^+$) followed by fixation and permeabilization using a commercially available FoxP3/transcription factor staining buffer kit according to the manufacturer's guidelines (eBioscience). At the permeabilization step, the cells were intracellularly stained with granzyme B-FITC and IFN-γ-APC. The cell proliferation rate was determined by Ki67 expression in permeabilized cells 24 h post-gB peptide stimulation using Ki67-Alexa Fluor 488 antibody. All labeled cells were acquired with a MacsQuant flow cytometer, and the exported FCS files were analyzed with FlowJo software. Determination of the polyfunctional phenotype of HSV gB-specific $CD8^+$ effector T cells was conducted using SPICE version 5.3 software (National Institute of Allergy and Infectious Diseases, National Institutes of Health) (103). Gating was confirmed using non-stimulated cells or fluorescence minus one controls.

Immunochemistry and confocal microscopy. Mice were euthanized and the eyes were removed at the indicated time p.i. All tissue preparation, antibody source and dilutions, and confocal imaging were as previously described (38).

Proangiogenic factor measurement. Corneas were collected from vaccinated gBT-I.1 mice at day 7 p.i., weighed, and homogenized in the presence of 1$\times$ Calbiochem protease inhibitor cocktail set I (EMD Millipore, Billerica, MA, USA) and tissue protein extraction reagent (TPER) (Thermo Fisher). The tissue homogenates were centrifuged at 10,000 $\times$ *g* for 1.5 min at 4°C. Supernatants were collected and assessed for angiopoietin (ANG)-2, fibroblast growth factor 2 (FGF-2, interleukin-6 (IL-6), and vascular endothelial growth factor A (VEGF-A) content using a bead-based multiplex assay for protein detection (Millipore Sigma).

Cornea opacity. Corneas were harvested from infected mice on day 7 p.i. and fixed with 4% paraformaldehyde for 30 min at room temperature, followed by washes (3$\times$) in 1 ml PBS (10 min per wash). The corneas were then immersed in glycerol 50% in PBS for 30 min. Each cornea was placed in the bottom and center of the well of a U-bottom, 96-well plate. The remaining glycerol was removed, and the corneas were incubated at room temperature for 10 min. Immediately prior to introducing the 96-well plate into the plate reader, 100 μl of glycerol 50% in PBS was slowly added to each well. The absorbance was measured at 500 nm using a CLARIOstar microplate reader (BMG Labtech, Ortenberg, Germany) using a 30 $\times$ 30 matrix as previously described (82).

ELiSPOT assay. For detection of IFN-γ using the ELISPOT assay, MultiScreen-IP sterile 96-well filtration plates (Millipore) were activated with 70% ethanol (100 μl/well) for 10 min at room temperature and then coated (5 μg/ml in PBS) with primary (capture) anti-mouse IFN-γ antibody (BD Biosciences). The plates were then incubated overnight at 4°C. TG single cell suspensions were plated into coated wells of 96-well flat-bottom plates and stimulated with 10 μg/ml of HSV-1 $gB_{498-505}$ peptide (SSIEFARL) overnight in a 37°C incubator (5% CO_2, 95% air). Next, the plates were extensively washed with distilled water and treated with blocking buffer (1% BSA in PBS) for 1 h at room temperature. Subsequently, the blocking buffer was removed and the plates were treated with secondary (detection) biotinylated anti-mouse IFN-γ antibody (2 μg/ml in 1% BSA/PBS) and streptavidin-alkaline phosphatase (1,000$\times$ diluted in 1%

BSA/PBS) for 1 h at room temperature. Finally, the plates were extensively washed with distilled water, and Sigma Fast BCIP/NBT (Sigma-Aldrich) was added. Plates were allowed to dry overnight and then were read with an ELISPOT reader (Cellular Technology Ltd.). The number of individual spots was determined using ImmunoSpot software (Cellular Technology Ltd.).

Metabolic flux assay. Oxygen consumption rates (OCR) and extracellular acidification rates (ECAR) were determined using a Seahorse XFe96 analyzer (Agilent) and Seahorse XF Cell Mito Stress and XF Glycolysis Stress kits, respectively. One day prior to running the assay, a sensor cartridge was hydrated with water overnight in a 37°C incubator without CO_2. The following day, water was removed and replaced with XF calibrant buffer followed by a 2- to 3-h incubation period at 37°C without CO_2. Mandibular lymph node cells (5×10^6 cells/2 ml) from vaccinated gBT-I.1 transgenic mice were prestimulated with 10 μg/ml of gB peptide for 48 h prior to metabolic flux assay in RPMI 1640 with 10% FBS in 12-well tissue culture plates (Nest Biotech Co. Ltd.). Following the incubation period, $CD8^+$ T cells were negatively selected using a CD8a T cell isolation kit (Miltenyi) achieving >95% enrichment. To evaluate the OCR, the gB peptide-pulsed cells were plated into Cell-Tak coated (22.4 μg/ml) 96-well plates (Agilent) at 3×10^6 cells per well in Seahorse XF RPMI medium containing 2 mM L-glutamine, 10 mM D-glucose, 1 mM sodium pyruvate, and 1 mM HEPES. The plate with seeded cells was degassed for 1 h at 37°C without CO_2 prior to starting the assay. OCR was measured before and after injecting 1.5 μM oligomycin, 1 μM carbonyl cyanide 4-(trifluoromethoxy) phenylhydrazone (FCCP), and 0.5 μM rotenone/antimycin A (AA). For the ECAR measurement, cells were prepared and plated as described above with the exception that the Seahorse XF RPMI medium did not contain 10 mM D-glucose. ECAR was measured before and after injection of 10 mM glucose, 2 μM oligomycin, and 50 mM 2-deoxy-glucose (2-DG). Basal OCR levels were determined as OCR values before injection of oligomycin. Baseline ATP production was determined by subtracting the average OCR values obtained after oligomycin administration from the average basal OCR values. Spare respiratory capacity was defined as the average OCR values after FCCP administration minus the average baseline OCR values. Aerobic glycolysis was determined by subtracting basal ECAR values from ECAR values after injection of glucose. Glycolytic capacity was calculated by subtracting 2-DG values from ECAR values after injection of oligomycin. All changes in metabolic flux were recorded in real time using Wave software version 2.6.1, and the data were analyzed using GraphPad Prism statistical software.

$CD8^+$ T cell depletion. HSV-1 0ΔNLS-vaccinated mice were treated with 200 μg rat anti-mouse CD8a IgG (Bio X Cell) rat IgG isotypic control subcutaneously 48 h prior to, 24 h prior to, and at the time of infection with HSV-1 (10^5 PFU/cornea). Three days p.i., mice were again treated with anti-CD8a or isotypic control IgG. Mice were monitored for survival out to day 30 p.i. Depletion of gB-specific $CD8^+$ T cells was confirmed (90 to 98% depletion) at the time of infection based on levels detected in the MLN, TG, and cornea.

Statistical analysis. Data are presented as the mean ± the standard error of the mean (SEM). Prism 8 software (GraphPad, San Diego, CA, USA) was used for statistical analysis, and the tests utilized to determined significance ($P < 0.05$) are described in each figure legend.

ACKNOWLEDGMENTS

This work was supported by NIH R01 AI053108, NEI core grant P30 EY021725, and an unrestricted grant from Research to Prevent Blindness.

We thank the staff of the Dean McGee Eye Institute animal facility for their efforts in maintaining and monitoring our mice. We thank Renee Sallack for technical assistance.

A.F., M.M., G.B.G., A.C., and D.J.R. have no conflicts of interest to report. D.J.J.C. is a member of the Scientific Advisory Board of Rational Vaccines, Inc., which has licensed U.S. patents 77856605 and 8802109 for the 0ΔNLS vaccine.

REFERENCES

1. Aldisi RS, Elsidiq MS, Dargham SR, Sahara AS, Al-Absi ES, Nofal MY, Mohammed LI, Abu-Raddad LJ, Nasrallah GK. 2018. Performance evaluation of four type-specific commercial assays for detection of herpes simplex virus type 1 antibodies in a Middle East and North Africa population. J Clin Virol 103:1–7. https://doi.org/10.1016/j.jcv.2018.03.011.
2. Khadr L, Harfouche M, Omori R, Schwarzer G, Chemaitelly H, Abu-Raddad LJ. 2019. The epidemiology of herpes simplex virus type 1 in Asia: systematic review, meta-analyses, and meta-regressions. Clin Infect Dis 68:757–772. https://doi.org/10.1093/cid/ciy562.
3. Sukik L, Alyafei M, Harfouche M, Abu-Raddad LJ. 2019. Herpes simplex virus type 1 epidemiology in Latin America and the Caribbean: systematic review and meta-analytics. PLoS One 14:e0215487. https://doi.org/10.1371/journal.pone.0215487.
4. Chemaitelly H, Nagelkerke N, Omori R, Abu-Raddad LJ. 2019. Characterizing herpes simplex virus type 1 and type 2 seroprevalence declines and epidemiological association in the United States. PLoS One 14:e0214151. https://doi.org/10.1371/journal.pone.0214151.
5. Patton ME, Bernstein K, Liu G, Zaidi A, Markowitz LE. 2018. Seroprevalence of herpes simplex virus types 1 and 2 among pregnant women and sexually active, nonpregnant women in the United States. Clin Infect Dis 67:1535–1542. https://doi.org/10.1093/cid/ciy318.
6. Korr G, Thamm M, Czogiel I, Poethko-Mueller C, Bremer V, Jansen K. 2017. Decreasing seroprevalence of herpes simplex virus type 1 and type 2 in Germany leaves many people susceptible to genital infection: time to raise awareness and enhance control. BMC Infect Dis 17:471. https://doi.org/10.1186/s12879-017-2527-1.
7. Fatahzadeh M, Schwartz RA. 2007. Human herpes simplex virus infections: epidemiology, pathogenesis, symptomatology, diagnosis, and management. J Am Acad Dermatol 57:737–763. quiz 764-6. https://doi.org/10.1016/j.jaad.2007.06.027.
8. Itzhaki RF. 2017. Herpes simplex virus type 1 and Alzheimer's disease: possible mechanisms and signposts. FASEB J 31:3216–3226. https://doi.org/10.1096/fj.201700360.
9. Eimer WA, Vijaya Kumar DK, Navalpur Shanmugam NK, Rodriguez AS,

Mitchell T, Washicosky KJ, Gyorgy B, Breakefield XO, Tanzi RE, Moir RD. 2018. Alzheimer's disease-associated beta-amyloid is rapidly seeded by herpesviridae to protect against brain infection. Neuron 100:1527–1532. https://doi.org/10.1016/j.neuron.2018.11.043.
10. De Chiara G, Piacentini R, Fabiani M, Mastrodonato A, Marcocci ME, Limongi D, Napoletani G, Protto V, Coluccio P, Celestino I, Li Puma DD, Grassi C, Palamara AT. 2019. Recurrent herpes simplex virus-1 infection induces hallmarks of neurodegeneration and cognitive deficits in mice. PLoS Pathog 15:e1007617. https://doi.org/10.1371/journal.ppat.1007617.
11. Ezzat K, Pernemalm M, Palsson S, Roberts TC, Jarver P, Dondalska A, Bestas B, Sobkowiak MJ, Levanen B, Skold M, Thompson EA, Saher O, Kari OK, Lajunen T, Sverremark Ekstrom E, Nilsson C, Ishchenko Y, Malm T, Wood MJA, Power UF, Masich S, Linden A, Sandberg JK, Lehtio J, Spetz AL, El Andaloussi S. 2019. The viral protein corona directs viral pathogenesis and amyloid aggregation. Nat Commun 10:2331. https://doi.org/10.1038/s41467-019-10192-2.
12. Whitley RJ. 2013. Changing epidemiology of herpes simplex virus infections. Clin Infect Dis 56:352–353. https://doi.org/10.1093/cid/cis894.
13. Ayoub HH, Chemaitelly H, Abu-Raddad LJ. 2019. Characterizing the transitioning epidemiology of herpes simplex virus type 1 in the USA: model-based predictions. BMC Med 17:57. https://doi.org/10.1186/s12916-019-1285-x.
14. Schaeffer HJ, Beauchamp L, de Miranda P, Elion GB, Bauer DJ, Collins P. 1978. 9-(2-hydroxyethoxymethyl) guanine activity against viruses of the herpes group. Nature 272:583–585. https://doi.org/10.1038/272583a0.
15. Vadlapudi AD, Vadlapatla RK, Earla R, Sirimulla S, Bailey JB, Pal D, Mitra AK. 2013. Novel biotinylated lipid prodrugs of acyclovir for the treatment of herpetic keratitis (HK): transporter recognition, tissue stability and antiviral activity. Pharm Res 30:2063–2076. https://doi.org/10.1007/s11095-013-1059-7.
16. Crute JJ, Grygon CA, Hargrave KD, Simoneau B, Faucher AM, Bolger G, Kibler P, Liuzzi M, Cordingley MG. 2002. Herpes simplex virus helicase-primase inhibitors are active in animal models of human disease. Nat Med 8:386–391. https://doi.org/10.1038/nm0402-386.
17. Kleymann G, Fischer R, Betz UA, Hendrix M, Bender W, Schneider U, Handke G, Eckenberg P, Hewlett G, Pevzner V, Baumeister J, Weber O, Henninger K, Keldenich J, Jensen A, Kolb J, Bach U, Popp A, Maben J, Frappa I, Haebich D, Lockhoff O, Rubsamen-Waigmann H. 2002. New helicase-primase inhibitors as drug candidates for the treatment of herpes simplex disease. Nat Med 8:392–398. https://doi.org/10.1038/nm0402-392.
18. Jaishankar D, Yakoub AM, Yadavalli T, Agelidis A, Thakkar N, Hadigal S, Ames J, Shukla D. 2018. An off-target effect of BX795 blocks herpes simplex virus type 1 infection of the eye. Sci Transl Med 10:eaan5861. https://doi.org/10.1126/scitranslmed.aan5861.
19. Velusamy T, Gowripalan A, Tscharke DC. 2020. CRISPR/Cas9-based genome editing of HSV. Methods Mol Biol 2060:169–183. https://doi.org/10.1007/978-1-4939-9814-2_9.
20. van Diemen FR, Kruse EM, Hooykaas MJ, Bruggeling CE, Schurch AC, van Ham PM, Imhof SM, Nijhuis M, Wiertz EJ, Lebbink RJ. 2016. CRISPR/Cas9-mediated genome editing of herpesviruses limits productive and latent infections. PLoS Pathog 12:e1005701. https://doi.org/10.1371/journal.ppat.1005701.
21. Oh HS, Neuhausser WM, Eggan P, Angelova M, Kirchner R, Eggan KC, Knipe DM. 2019. Herpesviral lytic gene functions render the viral genome susceptible to novel editing by CRISPR/Cas9. Elife 8:e51662. https://doi.org/10.7554/eLife.51662.
22. Nelson CE, Wu Y, Gemberling MP, Oliver ML, Waller MA, Bohning JD, Robinson-Hamm JN, Bulaklak K, Castellanos Rivera RM, Collier JH, Asokan A, Gersbach CA. 2019. Long-term evaluation of AAV-CRISPR genome editing for Duchenne muscular dystrophy. Nat Med 25:427–432. https://doi.org/10.1038/s41591-019-0344-3.
23. Maeder ML, Stefanidakis M, Wilson CJ, Baral R, Barrera LA, Bounoutas GS, Bumcrot D, Chao H, Ciulla DM, DaSilva JA, Dass A, Dhanapal V, Fennell TJ, Friedland AE, Giannoukos G, Gloskowski SW, Glucksmann A, Gotta GM, Jayaram H, Haskett SJ, Hopkins B, Horng JE, Joshi S, Marco E, Mepani R, Reyon D, Ta T, Tabbaa DG, Samuelsson SJ, Shen S, Skor MN, Stetkiewicz P, Wang T, Yudkoff C, Myer VE, Albright CF, Jiang H. 2019. Development of a gene-editing approach to restore vision loss in Leber congenital amaurosis type 10. Nat Med 25:229–233. https://doi.org/10.1038/s41591-018-0327-9.
24. Royer DJ, Cohen A, Carr D. 2015. The current state of vaccine development for ocular HSV-1 infection. Expert Rev Ophthalmol 10:113–126. https://doi.org/10.1586/17469899.2015.1004315.
25. Cremer KJ, Mackett M, Wohlenberg C, Notkins AL, Moss B. 1985. Vaccinia virus recombinant expressing herpes simplex virus type 1 glycoprotein D prevents latent herpes in mice. Science 228:737–740. https://doi.org/10.1126/science.2986288.
26. Keadle TL, Laycock KA, Miller JK, Hook KK, Fenoglio ED, Francotte M, Slaoui M, Stuart PM, Pepose JS. 1997. Efficacy of a recombinant glycoprotein D subunit vaccine on the development of primary and recurrent ocular infection with herpes simplex virus type 1 in mice. J Infect Dis 176:331–338. https://doi.org/10.1086/514049.
27. Inoue T, Inoue Y, Nakamura T, Yoshida A, Takahashi K, Inoue Y, Shimomura Y, Tano Y, Fujisawa Y, Aono A, Hayashi K. 2000. Preventive effect of local plasmid DNA vaccine encoding gD or gD-IL-2 on herpetic keratitis. Invest Ophthalmol Vis Sci 41:4209–4215.
28. Cha SC, Kim YS, Cho JK, Cho J, Kim SY, Kang H, Cho MH, Lee HH. 2002. Enhanced protection against HSV lethal challenges in mice by immunization with a combined HSV-1 glycoprotein B:H:L gene DNAs. Virus Res 86:21–31. https://doi.org/10.1016/s0168-1702(02)00037-0.
29. Awasthi S, Lubinski JM, Friedman HM. 2009. Immunization with HSV-1 glycoprotein C prevents immune evasion from complement and enhances the efficacy of an HSV-1 glycoprotein D subunit vaccine. Vaccine 27:6845–6853. https://doi.org/10.1016/j.vaccine.2009.09.017.
30. Hu K, Dou J, Yu F, He X, Yuan X, Wang Y, Liu C, Gu N. 2011. An ocular mucosal administration of nanoparticles containing DNA vaccine pRSC-gD-IL-21 confers protection against mucosal challenge with herpes simplex virus type 1 in mice. Vaccine 29:1455–1462. https://doi.org/10.1016/j.vaccine.2010.12.031.
31. Keadle TL, Morrison LA, Morris JL, Pepose JS, Stuart PM. 2002. Therapeutic immunization with a virion host shutoff-defective, replication-incompetent herpes simplex virus type 1 strain limits recurrent herpetic ocular infection. J Virol 76:3615–3625. https://doi.org/10.1128/JVI.76.8.3615-3625.2002.
32. Lu Z, Brans R, Akhrameyeva NV, Murakami N, Xu X, Yao F. 2009. High-level expression of glycoprotein D by a dominant-negative HSV-1 virus augments its efficacy as a vaccine against HSV-1 infection. J Invest Dermatol 129:1174–1184. https://doi.org/10.1038/jid.2008.349.
33. Randazzo BP, Kucharczuk JC, Litzky LA, Kaiser LR, Brown SM, MacLean A, Albelda SM, Fraser NW. 1996. Herpes simplex 1716—an ICP 34.5 mutant—is severely replication restricted in human skin xenografts in vivo. Virology 223:392–395. https://doi.org/10.1006/viro.1996.0493.
34. Franchini M, Abril C, Schwerdel C, Ruedl C, Ackermann M, Suter M. 2001. Protective T-cell-based immunity induced in neonatal mice by a single replicative cycle of herpes simplex virus. J Virol 75:83–89. https://doi.org/10.1128/JVI.75.1.83-89.2001.
35. Richards AL, Sollars PJ, Pitts JD, Stults AM, Heldwein EE, Pickard GE, Smith GA. 2017. The pUL37 tegument protein guides alpha-herpesvirus retrograde axonal transport to promote neuroinvasion. PLoS Pathog 13:e1006741. https://doi.org/10.1371/journal.ppat.1006741.
36. Davido DJ, Tu EM, Wang H, Korom M, Gazquez Casals A, Reddy PJ, Mostafa HH, Combs B, Haenchen SD, Morrison LA. 2018. Attenuated herpes simplex virus 1 (HSV-1) expressing a mutant form of ICP6 stimulates a strong immune response that protects mice against HSV-1-induced corneal disease. J Virol 92:e01036-18. https://doi.org/10.1128/JVI.01036-18.
37. Naidu SK, Nabi R, Cheemarla NR, Stanfield BA, Rider PJ, Jambunathan N, Chouljenko VN, Carter R, Del Piero F, Langohr I, Kousoulas KG. 2020. Intramuscular vaccination of mice with the human herpes simplex virus type-1(HSV-1) VC2 vaccine, but not its parental strain HSV-1(F) confers full protection against lethal ocular HSV-1 (McKrae) pathogenesis. PLoS One 15:e0228252. https://doi.org/10.1371/journal.pone.0228252.
38. Royer DJ, Gurung HR, Jinkins JK, Geltz JJ, Wu JL, Halford WP, Carr DJJ. 2016. A highly efficacious herpes simplex virus 1 vaccine blocks viral pathogenesis and prevents corneal immunopathology via humoral immunity. J Virol 90:5514–5529. https://doi.org/10.1128/JVI.00517-16.
39. Royer DJ, Carr MM, Chucair-Elliott AJ, Halford WP, Carr DJ. 2017. Impact of type I interferon on the safety and immunogenicity of an experimental live-attenuated herpes simplex virus 1 vaccine in mice. J Virol 9190:e02342-16. https://doi.org/10.1128/JVI.02342-16.
40. Royer DJ, Hendrix JF, Larabee CM, Reagan AM, Sjoelund VH, Robertson DM, Carr DJJ. 2019. Vaccine-induced antibodies target sequestered viral antigens to prevent ocular HSV-1 pathogenesis, preserve vision,

and preempt productive neuronal infection. Mucosal Immunol 12:827–839. https://doi.org/10.1038/s41385-019-0131-y.
41. Pereira RA, Simon MM, Simmons A. 2000. Granzyme A, a noncytolytic component of CD8(+) cell granules, restricts the spread of herpes simplex virus in the peripheral nervous systems of experimentally infected mice. J Virol 74:1029–1032. https://doi.org/10.1128/jvi.74.2.1029-1032.2000.
42. Liu T, Khanna KM, Chen X, Fink DJ, Hendricks RL. 2000. CD8(+) T cells can block herpes simplex virus type 1 (HSV-1) reactivation from latency in sensory neurons. J Exp Med 191:1459–1466. https://doi.org/10.1084/jem.191.9.1459.
43. Khanna KM, Bonneau RH, Kinchington PR, Hendricks RL. 2003. Herpes simplex virus-specific memory CD8+ T cells are selectively activated and retained in latently infected sensory ganglia. Immunity 18:593–603. https://doi.org/10.1016/s1074-7613(03)00112-2.
44. Banerjee K, Biswas PS, Kumaraguru U, Schoenberger SP, Rouse BT. 2004. Protective and pathological roles of virus-specific and bystander CD8+ T cells in herpetic stromal keratitis. J Immunol 173:7575–7583. https://doi.org/10.4049/jimmunol.173.12.7575.
45. Lang A, Nikolich-Zugich J. 2005. Development and migration of protective CD8+ T cells into the nervous system following ocular herpes simplex virus-1 infection. J Immunol 174:2919–2925. https://doi.org/10.4049/jimmunol.174.5.2919.
46. Sheridan BS, Khanna KM, Frank GM, Hendricks RL. 2006. Latent virus influences the generation and maintenance of CD8+ T cell memory. J Immunol 177:8356–8364. https://doi.org/10.4049/jimmunol.177.12.8356.
47. Knickelbein JE, Khanna KM, Yee MB, Baty CJ, Kinchington PR, Hendricks RL. 2008. Noncytotoxic lytic granule-mediated CD8+ T cell inhibition of HSV-1 reactivation from neuronal latency. Science 322:268–271. https://doi.org/10.1126/science.1164164.
48. Mueller SN, Heath W, McLain JD, Carbone FR, Jones CM. 2002. Characterization of two TCR transgenic mouse lines specific for herpes simplex virus. Immunol Cell Biol 80:156–163. https://doi.org/10.1046/j.1440-1711.2002.01071.x.
49. Wallace ME, Keating R, Heath WR, Carbone FR. 1999. The cytotoxic T-cell response to herpes simplex virus type 1 infection of C57BL/6 mice is almost entirely directed against a single immunodominant determinant. J Virol 73:7619–7626. https://doi.org/10.1128/JVI.73.9.7619-7626.1999.
50. Miller JK, Laycock KA, Umphress JA, Hook KK, Stuart PM, Pepose JS. 1996. A comparison of recurrent and primary herpes simplex keratitis in NIH inbred mice. Cornea 15:497–504.
51. Banerjee K, Biswas PS, Kim B, Lee S, Rouse BT. 2004. CXCR2-/- mice show enhanced susceptibility to herpetic stromal keratitis: a role for IL-6-induced neovascularization. J Immunol 172:1237–1245. https://doi.org/10.4049/jimmunol.172.2.1237.
52. Wuest TR, Carr DJ. 2010. VEGF-A expression by HSV-1-infected cells drives corneal lymphangiogenesis. J Exp Med 207:101–115. https://doi.org/10.1084/jem.20091385.
53. Pepose JS. 1991. Herpes simplex keratitis: role of viral infection versus immune response. Surv Ophthalmol 35:345–352. https://doi.org/10.1016/0039-6257(91)90184-h.
54. Yan XT, Tumpey TM, Kunkel SL, Oakes JE, Lausch RN. 1998. Role of MIP-2 in neutrophil migration and tissue injury in the herpes simplex virus-1-infected cornea. Invest Ophthalmol Vis Sci 39:1854–1862.
55. Meyers RL, Pettit TH. 1974. Chemotaxis of polymorphonuclear leukocytes in corneal inflammation: tissue injury in herpes simplex virus infection. Invest Ophthalmol 13:187–197.
56. Meyers RL, Chitjian PA. 1976. Immunology of herpesvirus infection: immunity to herpes simplex virus in eye infections. Surv Ophthalmol 21:194–204. https://doi.org/10.1016/0039-6257(76)90100-4.
57. Hendricks RL, Tumpey TM. 1990. Contribution of virus and immune factors to herpes simplex virus type l-induced corneal pathology. Invest Ophthalmol Vis Sci 31:1929–1939.
58. Niemialtowski MG, Rouse BT. 1992. Predominance of Th1 cells in ocular tissues during herpetic stromal keratitis. J Immunol 149:3035–3039.
59. St Leger AJ, Jeon S, Hendricks RL. 2013. Broadening the repertoire of functional herpes simplex virus type 1-specific CD8+ T cells reduces viral reactivation from latency in sensory ganglia. J Immunol 191:2258–2265. https://doi.org/10.4049/jimmunol.1300585.
60. Dervillez X, Qureshi H, Chentoufi AA, Khan AA, Kritzer E, Yu DC, Diaz OR, Gottimukkala C, Kalantari M, Villacres MC, Scarfone VM, McKinney DM, Sidney J, Sette A, Nesburn AB, Wechsler SL, BenMohamed L. 2013. Asymptomatic HLA-A*02:01-restricted epitopes from herpes simplex virus glycoprotein B preferentially recall polyfunctional CD8+ T cells from seropositive asymptomatic individuals and protect HLA transgenic mice against ocular herpes. J Immunol 191:5124–5138. https://doi.org/10.4049/jimmunol.1301415.
61. Vahed H, Agrawal A, Srivastava R, Prakash S, Coulon PA, Roy S, BenMohamed L. 2019. Unique type I interferon, expansion/survival cytokines, and JAK/STAT gene signatures of multifunctional herpes simplex virus-specific effector memory CD8(+) TEM cells are associated with asymptomatic herpes in humans. J Virol 93:e01882-18. https://doi.org/10.1128/JVI.01882-18.
62. Yasukawa M, Ohminami H, Arai J, Kasahara Y, Ishida Y, Fujita S. 2000. Granule exocytosis, and not the fas/fas ligand system, is the main pathway of cytotoxicity mediated by alloantigen-specific CD4(+) as well as CD8(+) cytotoxic T lymphocytes in humans. Blood 95:2352–2355. https://doi.org/10.1182/blood.V95.7.2352.
63. Betts MR, Brenchley JM, Price DA, De Rosa SC, Douek DC, Roederer M, Koup RA. 2003. Sensitive and viable identification of antigen-specific CD8+ T cells by a flow cytometric assay for degranulation. J Immunol Methods 281:65–78. https://doi.org/10.1016/s0022-1759(03)00265-5.
64. Menendez CM, Jinkins JK, Carr DJ. 2016. Resident T cells are unable to control herpes simplex virus-1 activity in the brain ependymal region during latency. J Immunol 197:1262–1275. https://doi.org/10.4049/jimmunol.1600207.
65. Campana D, Coustan-Smith E, Janossy G. 1988. Double and triple staining methods for studying the proliferative activity of human B and T lymphoid cells. J Immunol Methods 107:79–88. https://doi.org/10.1016/0022-1759(88)90012-9.
66. Pearce EL, Poffenberger MC, Chang CH, Jones RG. 2013. Fueling immunity: insights into metabolism and lymphocyte function. Science 342:1242454. https://doi.org/10.1126/science.1242454.
67. Geltink RIK, Kyle RL, Pearce EL. 2018. Unraveling the complex interplay between T cell metabolism and function. Annu Rev Immunol 36:461–488. https://doi.org/10.1146/annurev-immunol-042617-053019.
68. Pollizzi KN, Patel CH, Sun IH, Oh MH, Waickman AT, Wen J, Delgoffe GM, Powell JD. 2015. mTORC1 and mTORC2 selectively regulate CD8+ T cell differentiation. J Clin Invest 125:2090–2108. https://doi.org/10.1172/JCI77746.
69. Bernstein DI, Stanberry LR. 1999. Herpes simplex virus vaccines. Vaccine 17:1681–1689. https://doi.org/10.1016/s0264-410x(98)00434-4.
70. Institute of Medicine Committee to Study Priorities for Vaccine D. 2000. The National Academies Collection: Reports funded by National Institutes of Health. *In* Stratton KR, Durch JS, Lawrence RS (ed), Vaccines for the 21st century: a tool for decisionmaking. https://doi.org/10.17226/5501. National Academies Press, Washington, DC.
71. Srivastava R, Khan AA, Spencer D, Vahed H, Lopes PP, Thai NT, Wang C, Pham TT, Huang J, Scarfone VM, Nesburn AB, Wechsler SL, BenMohamed L. 2015. HLA-A02:01-restricted epitopes identified from the herpes simplex virus tegument protein VP11/12 preferentially recall polyfunctional effector memory CD8+ T cells from seropositive asymptomatic individuals and protect humanized HLA-A*02:01 transgenic mice against ocular herpes. J Immunol 194:2232–2248. https://doi.org/10.4049/jimmunol.1402606.
72. Srivastava R, Khan AA, Huang J, Nesburn AB, Wechsler SL, BenMohamed L. 2015. A herpes simplex virus type 1 human asymptomatic CD8+ T-Cell epitopes-based vaccine protects against ocular herpes in a "humanized" HLA transgenic rabbit model. Invest Ophthalmol Vis Sci 56:4013–4028. https://doi.org/10.1167/iovs.15-17074.
73. Srivastava R, Khan AA, Garg S, Syed SA, Furness JN, Vahed H, Pham T, Yu HT, Nesburn AB, BenMohamed L. 2017. Human asymptomatic epitopes identified from the herpes simplex virus tegument protein VP13/14 (UL47) preferentially recall polyfunctional effector memory CD44high CD62Llow CD8+ TEM cells and protect humanized HLA-A*02:01 transgenic mice against ocular herpesvirus infection. J Virol 91:e01793-16. https://doi.org/10.1128/JVI.01793-16.
74. Khan AA, Srivastava R, Chentoufi AA, Kritzer E, Chilukuri S, Garg S, Yu DC, Vahed H, Huang L, Syed SA, Furness JN, Tran TT, Anthony NB, McLaren CE, Sidney J, Sette A, Noelle RJ, BenMohamed L. 2017. Bolstering the number and function of HSV-1-specific CD8(+) effector memory T cells and tissue-resident memory T cells in latently infected trigeminal ganglia reduces recurrent ocular herpes infection and disease. J Immunol 199:186–203. https://doi.org/10.4049/jimmunol.1700145.
75. Firat H, Garcia-Pons F, Tourdot S, Pascolo S, Scardino A, Garcia Z, Michel

ML, Jack RW, Jung G, Kosmatopoulos K, Mateo L, Suhrbier A, Lemonnier FA, Langlade-Demoyen P. 1999. H-2 class I knockout, HLA-A2.1-transgenic mice: a versatile animal model for preclinical evaluation of antitumor immunotherapeutic strategies. Eur J Immunol 29:3112–3121. https://doi.org/10.1002/(SICI)1521-4141(199910)29:10<3112::AID-IMMU3112>3.0.CO;2-Q.
76. Hu J, Peng X, Schell TD, Budgeon LR, Cladel NM, Christensen ND. 2006. An HLA-A2.1-transgenic rabbit model to study immunity to papillomavirus infection. J Immunol 177:8037–8045. https://doi.org/10.4049/jimmunol.177.11.8037.
77. Wang K, Tomaras GD, Jegaskanda S, Moody MA, Liao HX, Goodman KN, Berman PW, Rerks-Ngarm S, Pitisuttithum P, Nitayapan S, Kaewkungwal J, Haynes BF, Cohen JI. 2017. Monoclonal antibodies, derived from humans vaccinated with the RV144 HIV vaccine containing the HVEM binding domain of herpes simplex virus (HSV) glycoprotein D, neutralize HSV infection, mediate antibody-dependent cellular cytotoxicity, and protect mice from ocular challenge with HSV-1. J Virol 91:e00411-17. https://doi.org/10.1128/JVI.00411-17.
78. Suryawanshi A, Mulik S, Sharma S, Reddy PB, Sehrawat S, Rouse BT. 2011. Ocular neovascularization caused by herpes simplex virus type 1 infection results from breakdown of binding between vascular endothelial growth factor A and its soluble receptor. J Immunol 186:3653–3665. https://doi.org/10.4049/jimmunol.1003239.
79. Yun H, Rowe AM, Lathrop KL, Harvey SA, Hendricks RL. 2014. Reversible nerve damage and corneal pathology in murine herpes simplex stromal keratitis. J Virol 88:7870–7880. https://doi.org/10.1128/JVI.01146-14.
80. Chucair-Elliott AJ, Zheng M, Carr DJ. 2015. Degeneration and regeneration of corneal nerves in response to HSV-1 infection. Invest Ophthalmol Vis Sci 56:1097–1107. https://doi.org/10.1167/iovs.14-15596.
81. Rao P, Suvas S. 2019. Development of inflammatory hypoxia and prevalence of glycolytic metabolism in progressing herpes stromal keratitis lesions. J Immunol 202:514–526. https://doi.org/10.4049/jimmunol.1800422.
82. Filiberti A, Gmyrek GB, Montgomery ML, Sallack R, Carr DJJ. 2020. Loss of osteopontin expression reduces HSV-1-induced corneal opacity. Invest Ophthalmol Vis Sci 61:24. https://doi.org/10.1167/iovs.61.10.24.
83. Staats HF, Oakes JE, Lausch RN. 1991. Anti-glycoprotein D monoclonal antibody protects against herpes simplex virus type 1-induced diseases in mice functionally depleted of selected T-cell subsets or asialo GM1+ cells. J Virol 65:6008–6014. https://doi.org/10.1128/JVI.65.11.6008-6014.1991.
84. Metcalf JF, Koga J, Chatterjee S, Whitley RJ. 1987. Passive immunization with monoclonal antibodies against herpes simplex virus glycoproteins protects mice against herpetic ocular disease. Curr Eye Res 6:173–177. https://doi.org/10.3109/02713688709020086.
85. Conrady CD, Zheng M, Stone DU, Carr DJ. 2012. CD8+ T cells suppress viral replication in the cornea but contribute to VEGF-C-induced lymphatic vessel genesis. J Immunol 189:425–432. https://doi.org/10.4049/jimmunol.1200063.
86. Biswas PS, Banerjee K, Kinchington PR, Rouse BT. 2006. Involvement of IL-6 in the paracrine production of VEGF in ocular HSV-1 infection. Exp Eye Res 82:46–54. https://doi.org/10.1016/j.exer.2005.05.001.
87. Bryant-Hudson KM, Gurung HR, Zheng M, Carr DJ. 2014. Tumor necrosis factor alpha and interleukin-6 facilitate corneal lymphangiogenesis in response to herpes simplex virus 1 infection. J Virol 88:14451–14457. https://doi.org/10.1128/JVI.01841-14.
88. Royer DJ, Carr DJ. 2016. A STING-dependent innate-sensing pathway mediates resistance to corneal HSV-1 infection via upregulation of the antiviral effector tetherin. Mucosal Immunol 9:1065–1075. https://doi.org/10.1038/mi.2015.124.
89. Geiger KD, Nash TC, Sawyer S, Krahl T, Patstone G, Reed JC, Krajewski S, Dalton D, Buchmeier MJ, Sarvetnick N. 1997. Interferon-gamma protects against herpes simplex virus type 1-mediated neuronal death. Virology 238:189–197. https://doi.org/10.1006/viro.1997.8841.
90. Cantin E, Tanamachi B, Openshaw H. 1999. Role for gamma interferon in control of herpes simplex virus type 1 reactivation. J Virol 73:3418–3423. https://doi.org/10.1128/JVI.73.4.3418-3423.1999.
91. Lekstrom-Himes JA, LeBlanc RA, Pesnicak L, Godleski M, Straus SE. 2000. Gamma interferon impedes the establishment of herpes simplex virus type 1 latent infection but has no impact on its maintenance or reactivation in mice. J Virol 74:6680–6683. https://doi.org/10.1128/jvi.74.14.6680-6683.2000.
92. Liu T, Khanna KM, Carriere BN, Hendricks RL. 2001. Gamma interferon can prevent herpes simplex virus type 1 reactivation from latency in sensory neurons. J Virol 75:11178–11184. https://doi.org/10.1128/JVI.75.22.11178-11184.2001.
93. Tang R, Rangachari M, Kuchroo VK. 2019. Tim-3: a co-receptor with diverse roles in T cell exhaustion and tolerance. Semin Immunol 42:101302. https://doi.org/10.1016/j.smim.2019.101302.
94. Zhang Y, Ertl HC. 2014. The effect of adjuvanting cancer vaccines with herpes simplex virus glycoprotein D on melanoma-driven CD8+ T cell exhaustion. J Immunol 193:1836–1846. https://doi.org/10.4049/jimmunol.1302029.
95. McLane LM, Abdel-Hakeem MS, Wherry EJ. 2019. CD8 T cell exhaustion during chronic viral infection and cancer. Annu Rev Immunol 37:457–495. https://doi.org/10.1146/annurev-immunol-041015-055318.
96. Roy S, Coulon PG, Prakash S, Srivastava R, Geertsema R, Dhanushkodi N, Lam C, Nguyen V, Gorospe E, Nguyen AM, Salazar S, Alomari NI, Warsi WR, BenMohamed L. 2019. Blockade of PD-1 and LAG-3 immune checkpoints combined with vaccination restores the function of antiviral tissue-resident CD8(+) TRM cells and reduces ocular herpes simplex infection and disease in HLA transgenic rabbits. J Virol 93:e00827-19. https://doi.org/10.1128/JVI.00827-19.
97. Heldwein EE, Lou H, Bender FC, Cohen GH, Eisenberg RJ, Harrison SC. 2006. Crystal structure of glycoprotein B from herpes simplex virus 1. Science 313:217–220. https://doi.org/10.1126/science.1126548.
98. Sattentau Q. 2008. Avoiding the void: cell-to-cell spread of human viruses. Nat Rev Microbiol 6:815–826. https://doi.org/10.1038/nrmicro1972.
99. Orr MT, Orgun NN, Wilson CB, Way SS. 2007. Cutting edge: recombinant Listeria monocytogenes expressing a single immunedominant peptide confers protective immunity to herpes simplex virus-1 infection. J Immunol 178:4731–4735. https://doi.org/10.4049/jimmunol.178.8.4731.
100. Bauer D, Alt M, Dirks M, Buch A, Heilingloh CS, Dittmer U, Giebel B, Gorgens A, Palapys V, Kasper M, Eis-Hubinger AM, Sodeik B, Heiligenhaus A, Roggendorf M, Krawczyk A. 2017. A therapeutic antiviral antibody inhibits the anterograde directed neuron-to-cell spread of herpes simplex virus and protects against ocular disease. Front Microbiol 8:2115. https://doi.org/10.3389/fmicb.2017.02115.
101. Royer DJ, Zheng M, Conrady CD, Carr DJ. 2015. Granulocytes in ocular HSV-1 infection: opposing roles of mast cells and neutrophils. Invest Ophthalmol Vis Sci 56:3763–3775. https://doi.org/10.1167/iovs.15-16900.
102. Gurung HR, Carr MM, Bryant K, Chucair-Elliott AJ, Carr DJ. 2018. Fibroblast growth factor-2 drives and maintains progressive corneal neovascularization following HSV-1 infection. Mucosal Immunol 11:172–185. https://doi.org/10.1038/mi.2017.26.
103. Roederer M, Nozzi JL, Nason MC. 2011. SPICE: exploration and analysis of post-cytometric complex multivariate datasets. Cytometry A 79:167–174. https://doi.org/10.1002/cyto.a.21015.